UNIVERSITI TEKNIKAL MALAYSIA MELAKA

FACULTY OF ELECTRICAL ENGINEERING

BEKU 4894

FINAL YEAR PROJECT

REPORT

DYNAMIC MODELING OF A DOUBLE-PENDULUM GANTRY CRANE SYSTEM

NAME	:	NOOR FATIHA BINTI OMAR
COURSE	:	4 BEKC
SESSION	:	2013/2014
MATRIX NO	:	B011110149
LECTURER'S NAME	:	EN. HAZRIQ IZZUAN BIN JAAFAR

18th JUNE 2014

DYNAMIC MODELING OF A DOUBLE-PENDULUM GANTRY CRANE SYSTEM

NOOR FATIHA BINTI OMAR

A report submitted in partial fulfillment of the requirements for the degree of Bachelor of Electrical Engineering (Control, Instrumentation and Automation)

Faculty of Electrical Engineering

UNIVERSITI TEKNIKAL MALAYSIA MELAKA

2014

To my beloved mother and father

ACKNOWLEDGEMENT

Firstly, I would like to express my gratitude and appreciation to all those who gave me the possibility to complete this report. Deepest thanks to my supervisor, Encik Hazriq Izzuan Bin Jaafar for his invaluable guidance, stimulating suggestions and encouragement to complete this project. During under his supervision, lot of valuable information is obtained in order to coordinate and complete this project and thesis in the time given.

Special thanks and higher appreciation to my parents, family and special mate of mine for their cooperation, constructive suggestion and also supports from the beginning until the ends during the period of the project. Also thanks to all of my friends and others, that has been contributed by supporting and helps myself during the final year project progress till it is fully completed.

Last but not least, greater appreciation to BEKC Classmates and Electrical Engineering Faculty UTeM for great commitment and cooperation during my Final Year Project. Besides, I would like to appreciate the guidance given by the panels especially in our project presentation that has improved our presentation skills by their comment and tips.

ABSTRACT

This project presents investigations of dynamic behavior of Double Pendulum Gantry Crane System (DPGCS). The dynamic model system is developed and derived using Lagrange equation. The effects of performances in term of movement of the trolley and payload oscillation of the system are analyzed and discussed. The dynamic model is developed and the extensive results based on derivation are presented in the frequency domains. Simulation results are presented within MATLAB environment to verify the response performances of the system. It shows that several factors may affecting the performance of the DPGCS in terms of hook and load length, input force, hook mass, payload mass and trolley mass.

ABSTRAK

Projek ini membentangkan tentang kajian terhadap tingkah laku dinamik *Double-Pendulum Gantry Sistem Crane* (DPGCS). Sistem model dinamik diperolehi dengan menggunakan persamaan Lagrange. Kesan perubahan dari segi pergerakan troli dan ayunan beban dianalisa dan dibincangkan. Model dinamik juga dikaji dan keputusan yang diperolehi dipersembahkan dalam bentuk frekuensi domain. Keputusan simulasiyang dihasilkan melalui MATLAB adalah untuk mengkaji prestasi sistem tersebut. Ia menunjukkan bahawa beberapa faktor boleh menjejaskan prestasi DPGCS dari segi perubahan pada panjang kabel cangkuk dan kabel beban, kuasa input, muatan cangkuk, muatan beban dan muatan troli.

TABLE OF CONTENTS

LIST OF TABLES

LIST OF FIGURES

LIST OF ABBREVIATIONS

DPGCS	-	Double-Pendulum Gantry Crane System
GCS	-	Gantry Crane System

LIST OF SYMBOLS

m_1	-	Hook Mass
m_2	-	Payload Mass
m_3	-	Trolley Mass
L_1	-	Hook Pendulum Length
L_2	-	Load Pendulum Length
g	-	Gravity Acceleration
F	-	Bang-bang Force Input
x (m)	-	Trolley Displacement
θ_1	-	Hook Swing Angle
θ_2	-	Load Swing Angle
kg	-	Kilogram (Mass unit)
N	-	Newton (Force unit)
m	-	Meter (Distance unit)

LIST OF APPENDICES

CHAPTER 1

INTRODUCTION

1.0 Overview

This chapter will be discussed about the Gantry Crane System (GCS) dynamic analysis. The project objective, problem statement, scopes of work and methodology will also be presented in this chapter.

1.1 Gantry Crane System

By the centuries, humans have been facing a problem in lifting and handling heavy materials. There is no other way in solving the problem until the GCS has been introduced. The use of modern machine technology is a step to provide support in the construction, transportation and make daily life become more convenient. The industrial use of GCS are increasing with the demand for greater safety and faster transferring payloads. The uncontrolled payload motions that are suspended will become dangerous if accident occur along transferring payloads. Crane operators must be skilled in handling cranes and have the appropriate training to control the crane with more secure. The operator have the responsibility to plan carefully and taken the inspection before controlling the crane.

Thus, GCS supports to hold the load at a fixed location to move left or right and high or low. It consists of two or more legs parallel to each other on the bridge as shown in Figure 1.1. The heights of loads are depending on the maximum hook height. Samson and the Goliath have built the largest GCS ever that could each lift up to 840 tons [16].

Figure 1.1: Industrial Gantry Crane System (GCS)

Many cranes facing the same problem of the inefficiency cause by payload oscillations. It is difficult to manipulate payload accurately, quickly and safely because of the natural sway of crane payload. The purpose of crane controlling is to transfer the load as fast as possible without increasing any excessive sway at the desired position. Moreover, the results in a sway motion gave the terrible response when payload stopped after desired motion. The problem is become more complicated when the payload use a Double-Pendulum Gantry Crane System (DPGCS). It motion is very complex and its dynamic behavior are definitely related to the noise level of whole structure [10]. If the crane behaves like a single-pendulum, the crane operators can eliminate much of the residual motion by causing a deceleration oscillation that cancel the oscillation induced during acceleration. For the system that behaves like a double pendulum, manual method of eliminating residual vibration becomes very difficult even for the most experienced operators. It may cause an accident if the problem cannot be resolved.

1.2 Motivation

Safety issues are very important because the GCS involved the use of shipping heavy loads. Gantry crane accidents have the potential to cause a serious injury or death to employees and other person involved. Many cases have been reported involving an accident on the gantry crane. This accident occurred is due to failure in handling the crane and may cause load collapse. Even though the person that have been injured in accidents have the legal right to claim compensation for the losses if cause by the negligence of the employer but precaution is better to avoid the injury occurred.

This matter can be supported with incident occurred involving crane which is on May 21, 2013 (Tuesday) at the Gallatin, Tennessee where the crane (Terex/American 165) owned and operated by Mountain States Contractors. According to the inspection report, a construction worker died on previous works. During the incident happen, the crane was collapse and fall on to a moving car. In this accident, nobody was seriously hurt on Highway 109 in Gallatin when the crane was crashed down the car. Gallatin police reported that the strong winds at that time in the afternoon were caused of the accident.

Based on the above issues, another way to curb and prevent this problem from continuing to happens is to study the behavior of cranes system in order to analyze the response performance of the system.

Figure 1.2: The overview of crane accident.

1.3 Problem Statement

i. Gantry crane has been developed to transfer heavy load as fast as possible or in a short period of time without causing any excessive swing at the desired position. However, the trolley acceleration always induces unwanted load swing. If the mass of trolley were increased, swing angle becomes larger. It requires more time to minimize the swing angle.

ii. Most of the gantry crane is manually controlled by the skillful and experience operators in handling cranes in order to make sure the payload stop swaying at correct position. A manual control is one of the factors that cause an accident in case of carelessness in handling the cranes. If the load becomes larger, it may cause accident and also harm people surrounding.

1.4 Significant of Project

i. According to previous researches, a lot of controllers have been designed in order to find the good performance of DPGCS. Most of controllers are used to control the trolley position and payload oscillation. However, the expected result still cannot be solved.

ii. Most industries are used general controller such as PID, Fuzzy Logic, and Input Shaping to overcome and improve the performance response. By development and investigations of dynamic modeling, it will lead us to better understand the behavior DPGCS in terms of performance response.

1.5 Objectives of Project

There are two objectives to be achieved and listed for this project:

- To study the behavior performances of Double-Pendulum Gantry Crane System in terms of position, hook swing and payload swing.
- To investigate the effects on the dynamic behavior of a Double-Pendulum Gantry Crane System with different parameter values of input, hook length, load length, hook mass, payload mass and trolley mass.

1.6 Scopes of Project

In order to ensure this project is conducted within the boundary, three scopes are listed.

- Develop the double-pendulum model using MATLAB and Simulink
- Apply the bang-bang input in order to analyze the response performance and the simulation.
- Observation based on six criteria needed which is hook length, load length, input force, hook mass, payloads mass and trolley mass.

1.7 Project Report Outline

In this section, the outlines of project report were presented. This report is including of six chapters and each chapter is explained generally.

Chapter 1 generally discusses on introduction regarding to the dynamic modeling of DPGCS. The problem statement, objectives and significant of project are stated briefly and clearly.

Chapter 2 discusses the literature review on DPGCS. The improvement DPGCS are stated and reviewed based on previous researcher from 1998-2013.

Chapter 3 is discussed more about the methodology of DPGCS. The flow charts of project are listed by following the sequence in phase 1 and phase 2.

Chapter 4 is explained more about the mathematical expression that is used in the project. The dynamic modeling of DPGCS is referring to the previous published paper and journal. The derivations are clearly listed using the Lagrangian method.

Chapter 5 is representing the analysis of result by consist of two phase states in flow chart. In the first phase, the analysis results are express which involved the response of trolley displacement and the swing angle. The second phase involves the analysis of various parameters of force input, hook and load length, hook mass, payloads and trolley mass.

Chapter 6 is contained the conclusions on the whole project done and also the recommendation for improving the future works.

CHAPTER 2

LITERATURE REVIEW

2.0 Overview

In this chapter the review from previous research will be provided which is related to Double-Pendulum Gantry Crane System (DPGCS). The previous research is based on tuning method with difference type of controller in order to obtain the performance of gantry crane. All cranes share the same important limitation on efficiency which is the payload oscillation. Given the significance of cranes, a large amount of research has been provided and dedicated to eliminate the oscillation. A lot of researcher has been implement feedback control methods. The other solutions that researcher always use to reduce the oscillation are by using the command-shaping methods.

2.1 Previous Research on Development of Controller

In order to optimize the performance of double-pendulum gantry crane, several methods had been used in previous research. In [1], a robust nonlinear controller of cranes based on variable structural control approaches is developed. It used both conventional sliding mode control (CSMC) and its modified version, hierarchical sliding mode control (HSMC). The purposes of the study are to design a CSMC-based controller that can force trolley to move the desired position and hook swing angles to vanish completely at destination. However, this technique will chatter the control signal. The sign function is replaced with a saturation function to avoid the chattering control signal in CSMC. By replacing the sign function, this will sacrifice for the steady-state tracking accuracy of system responses.

On the different way, [3] have been developed wave-based control (WBC) to determine and achieve controlled motion of the load and at the same time moving the trolley to follow the required position while control the payload swing. By represents the flexible 3-D dynamic modeling of a gantry crane, WBC allows the trolley to reach a better performance in terms of load control.

To find the best solution of controller development, more researchers are trying to make a lot of research in case to find the best technique to control the payload. For [4], it try to implement the effectiveness of input shaping presents the effects of double-pendulum type overhead crane (DPTOC). This method focuses on the application of input shaping schemes to reduce a hook and load sway motion. It investigates the development of input shaping to control swaying of a DPTOC system. Experimental results demonstrated that it provide a higher level of swing reduction and the speed of response is slightly improved over settling time at the expense of solving a decrease in the level of sway reduction. It is concluded that the experiment results on DPTOC system has demonstrated the effectiveness and practicality of the proposed approach in reducing the sway motion of crane system.

Many researchers have studied this type of controller which is developed by [6]. It constructs the hybrid controller which included regulation of position and anti-swing control. Furthermore, a fuzzy LQR controller is designed using linear quadratic regulation according to linear system. With this controller, the position error and swing angle are achieved and it demonstrates the effectiveness of the controller to stable.

The other researcher, [8] also implement a hybrid controller include regulation of position and anti-swing control. It used the Takagi-Sugeno fuzzy model which using a fuzzy controller which designed using parallel distributed compensation and Linear Quadratic Regulation (LQR) [8]. The result reaches the final values of position and payload sway and the simulation also indicates the stability of overhead crane.

In addition, researcher [9] developed a numerous feedback based control methods and two-mode input command-shaping methods. Both methods reduced average task completion time from the manually controlled case. However, input shaping gives the lowest average completion time and also allow the operator to move the trolley on a shorter total path length to completing the tasks. The input shaping was more save the energy compared to feedback and manual control methods.

Furthermore, the researcher [11] presents to control schemes in tracking of trajectory and anti-sway system control. By using the method of Single Input Fuzzy Logic Controller (SIFLC) will decrease the conventional two-input FLC (CFLC) into a single input single output (SISO) controller. The performances of control are studied based influence of input tracking capability sway angle reduction angle compared to the control time response SIFLC. As for result, higher numbers of input sharper modes in SIFLC control are producing greater level of sway reduction compared to the lower input sharper modes. In case of lower number modes, the time responses also have been improved.

Researcher [12] explores the problems of gantry crane with using feedback for crane control. The problem includes the crane payload sensing difficulties, wide varying system dynamics, and compatibility of human operator. By using input shaping the favorable solution can be reached. Input shaping is another control method that can be used to eliminate crane payload oscillations. It can be made robust to varying system dynamics.

The composite sliding mode function (CSMF) methods are using by researcher [14] that using three sliding mode functions that to decouple the double-pendulum-type overhead crane (DPTOC). It presents the ways of determining the whole response of dynamic performance. The proposed of this controller are to greatly reduce the complexity for under-actuated systems. The SMC will analyze the concept of stability and performed the effectiveness of the proposed system.

The researcher from China, [15] designed the sliding mode fuzzy control methods that are presents in double-pendulum-type overhead crane. These methods allow in reducing the rules of fuzzy controller and use some method of adjustment of sliding mode controller. This method produced a greater result and initial condition will be not affected the performance.

One method for developing optimal controls is by using the command shaping method. Researcher [17] presents a method by using the command shaping method to improve the robustness and at the same time it will eliminate the crane oscillation. This method applies the dynamics of double-pendulum system in order to determine the input shaping parameters. However, by using the command shaping method it will introduces delay between the step and the start of system control. This happen when the systems are reacting on new reference steps and automatically a new reference computed.

In case of the research made from [18], a simple command shaping method is implemented to obtain results that verify the utility. These methods are adjusted to handle dynamics of double-pendulum better. The results shown oscillation changes slowly when the parameter changing. Input shaping became greater effective at the low mode. Because of the high dependence, robust shaper must be used for the second mode of system parameters.

Table 2.1: Summary for the type of technique use in years (1998-2013)

Year	Type of Controller	Researcher
2013	CSMC and HSMC [1]	Le Anh Tuan and Soon-Geul Lee *et. al*
2012	WBC [3]	W.O'Connor and H. Habibi *et. al*
2011	Fuzzy LQR [6]	Mahdieh Adeli *et. al*
2011	Closed-form equation [7]	R.M.T. Raja Ismail *et. al*
2011	Fuzzy LQR [8]	Mahdieh Adeli *et. al*
2011	Feedback based control and command-shaping [9]	Ajeya Karajgikar *et. al*
2010	SIFLC [11]	M.A. Ahmad, *et. al*
2010	Input Shaping [12]	Joshua Vaughan *et. al*
2005	CSMF [14]	Dian-Tong Liu *et. al*
2004	Sliding mode fuzzy control [15]	Dian-Tong Liu *et. al*
1999	Command shaping method [17]	Michael Kenison *et. al*
1998	Command shaping method [18]	William E. Singhose *et. al*

2.2 Previous Research on Dynamical Behavior

Recently, several investigations have been conducted to optimize the performance of GCS. In order to minimize the performance response of the payload swing and position, there are several researches about dynamical behavior of gantry crane. Founded that, [2] have been investigates the dynamic behavior of nonlinear GCS to verify the response of performance system. Various parameters of the system are tested to observing the behavior of the dynamic model system. With analyze this system, it is beneficial to the development of industry control.

Researcher [10] was developed the dynamic behaviors of double pendulum system. It introduced the behavior of double-pendulum by using certain system parameters at varying initial conditions. The double-pendulum behaviors are derived using Lagrangian equation and numerical computations. The result using numerical computations shows that the system may have different oscillation when the initial conditions were changes. It provides the result based on the characteristics and optimal design of the model.

In [13], present a 3-D dynamic modeling of a gantry crane system by using the closed-form equations. The dynamic model of the system will be derived using the Lagrangian method. It studied the impact of the payload response of system. The trolley position and swing angle responses are obtained. As result, the effects of payload characteristic are effective to control system with varying payload.

Table 2.2: Research of dynamic modeling (2009-2013)

Year	**Dynamic Modeling**	**Researcher**
2013	Nonlinear dynamic behavior of gantry crane system (single-pendulum) [2]	Hazriq Izzuan Jaafar *et. al*
2011	Nonlinear dynamic behavior of double-pendulum [10]	Chen Li-jie *et. al*
2009	3D dynamic modeling of double-pendulum gantry crane [13]	R.M.T. Raja Ismail *et. al*

CHAPTER 3

METHODOLOGY

3.0 Overview

In this chapter the main topics that will be discussed is the methodology and approach used to complete this project. A dynamic modeling is stated in this chapter according to the previous researcher.

3.1 Project Flow Chart

Figure 3.1 show the project flow chart that use to make sure this project is successfully done before the due date of this project:

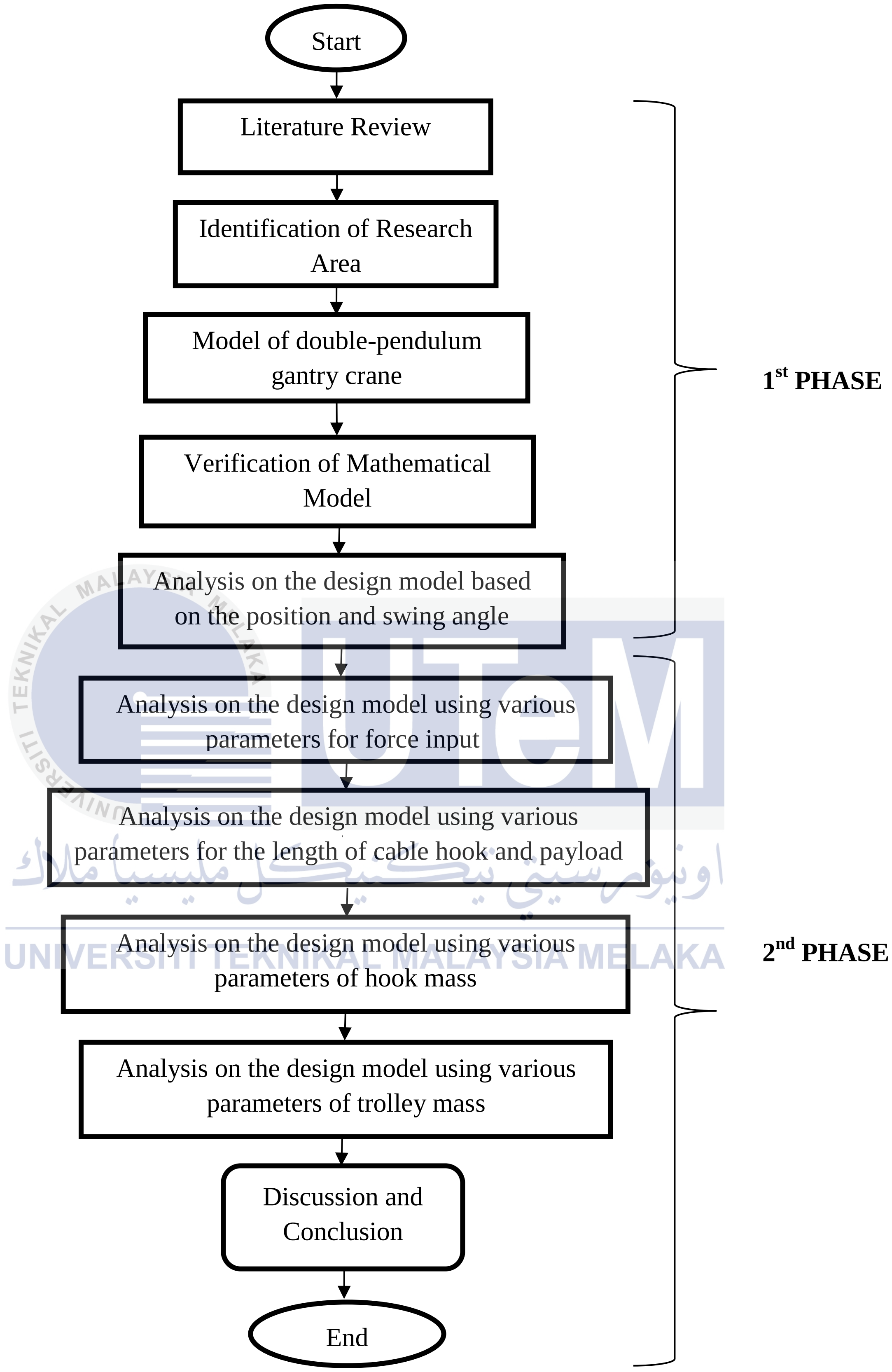

Figure 3.1: Flow Chart for the methodology of the Project

3.2 Lagrangian Equation

The Lagrangian equation is been developed by Joseph-Louis Lagrange (1736-1813) which provides to solve the motion in systems. One of the advantages of lagrangian is this equation will avoiding some constrains that holds the system together. By using this method it immediately will reducing problem in term of characteristic sizing. This equation result is presented in the differential equations which describes the motion equation of system.

- Lagrangian function:

$$L = T - V \tag{3.1}$$

T = Kinetic energies

V = Potential energies

- Lagrangian equation:

$$\frac{d}{dt}\left[\frac{\partial L}{\partial \dot{q}i}\right] - \frac{\partial L}{\partial qi} = Qi \tag{3.2}$$

3.3 Bang-bang Input Solution

Bang-bang input is a kind of feedback controller that used to switch dramatically between two points of input. Bang-bang input is characterized by turning the control element fully ON or fully OFF to regulate the average value of the parameter to be controlled. ON-OFF control is using higher limit and lower limit to bound input signal. The output signal will be oscillation around the given set-point.

In this project, a bang-bang force input has a positive which referring the acceleration and negative as referring the deceleration of period allowing the trolley to initially accelerate, decelerate and then stop at the desired location.

Figure 3.2: Bang-bang Input Force

CHAPTER 4

MODELING OF A DOUBLE-PENDULUM GANTRY CRANE SYSTEM

4.0 Overview

This chapter will be describing about the modeling of Double-Pendulum Gantry Crane System (DPGCS). In this chapter includes all the parameters needed in order to study the behavior of DPGCS. The Lagrangian function derived also presented.

4.1 Model of DPGCS

The payloads sway can create dynamic effects to control the performance. The payload configurations are creating double-pendulum effects. In these circumstances, the controller is now responsible for suppressing two modes of oscillation. If the control system is designed only for the single-pendulum payload system, then this can create significant problems which may include instability. If the double-pendulum is considered, then the result of controller will be more conservative for efficient operation with single-pendulum system.

In Figure 4.1, model of DPGCS is been selected. Nonlinear model of the DPGCS is modeled based on [7]. The x stands for the cart position while m_1, m_2 and m_3 respectively the hook mass, payload mass and trolley mass. The θ_1 is the hook swing angle and θ_2 is the load swing angle. The l_1 is the crane trolley through flexible cable length while l_2 is the load that attached to the hook with massless.

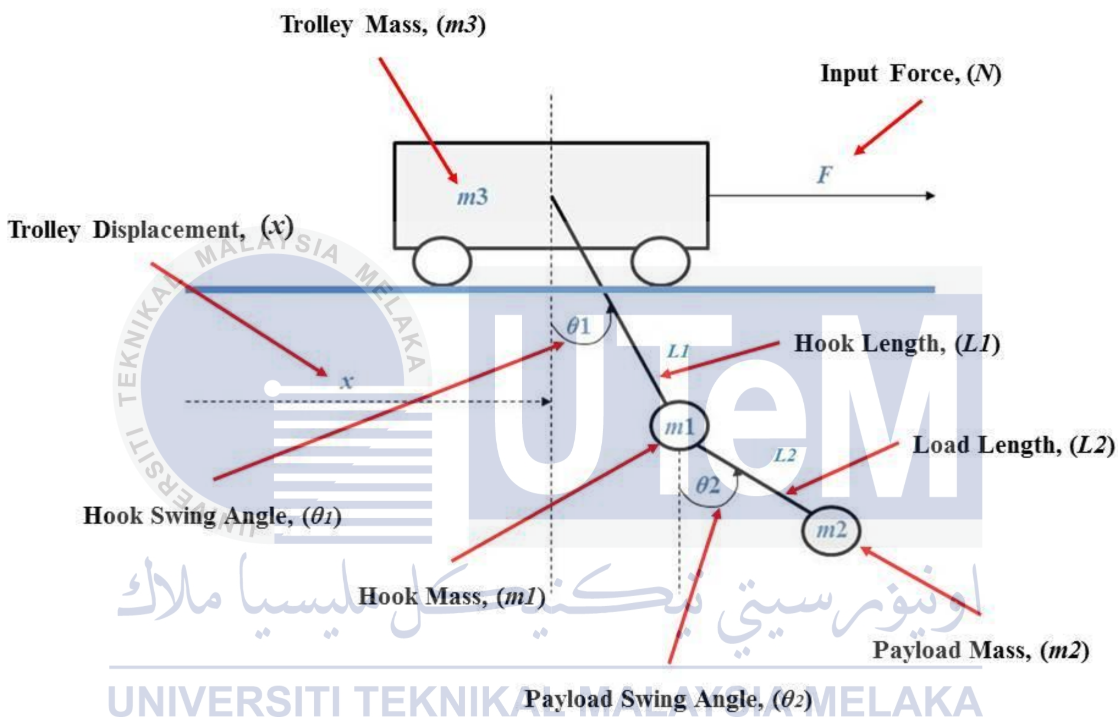

Figure 4.1: Description of the Double-Pendulum Gantry Crane System

Table 4.1: Parameter of the DPGCS

	Parameters	**Value**
m_1	Hook mass	2 kg
m_2	Payload mass	1-10 kg
m_3	Trolley mass	5 kg
L_1	Hook pendulum length	2 m
L_2	Load pendulum length	1 m
g	Gravity acceleration	9.8 m-s^{-2}
F	Bang-bang force input	5 N (amplitude) / 1 s (width)

Table 4.2: The variable of the system

Symbol	**Variable**	**Desired Output**
x (m)	Trolley Displacement	To achieve steady state position with minimum error
θ_1 **(rad)**	Hook swing angle	To avoid excessive swing at hook
θ_2 **(rad)**	Load swing angle	To avoid excessive swing at load

4.2 Mathematical Modeling of DPGCS

There are several method can be used to model the DPGCS. From the investigations, found that the Lagrange's Equation is more suitable to derive the mathematical expression for the modeling system. The double-pendulum system has three independent generalized coordinates namely trolley displacement (x), hook oscillation (θ_1) and payload oscillation (θ_2). The form for Lagrange's is given as:

$$\frac{d}{dt}\left[\frac{\partial L}{\partial \dot{q}_i}\right] - \frac{\partial L}{\partial q_i} = Q_i = F \tag{4.1}$$

Where q is for state vector and F is for the control vector

$$q = [x \quad \theta_1 \quad \theta_2] \tag{4.1.1}$$

$$F = [F \quad 0 \quad 0] \tag{4.1.2}$$

For L, Q_i and q_i is representing Lagrangian function. The Lagrangian function can be written as:

$$L = T - V \tag{4.2}$$

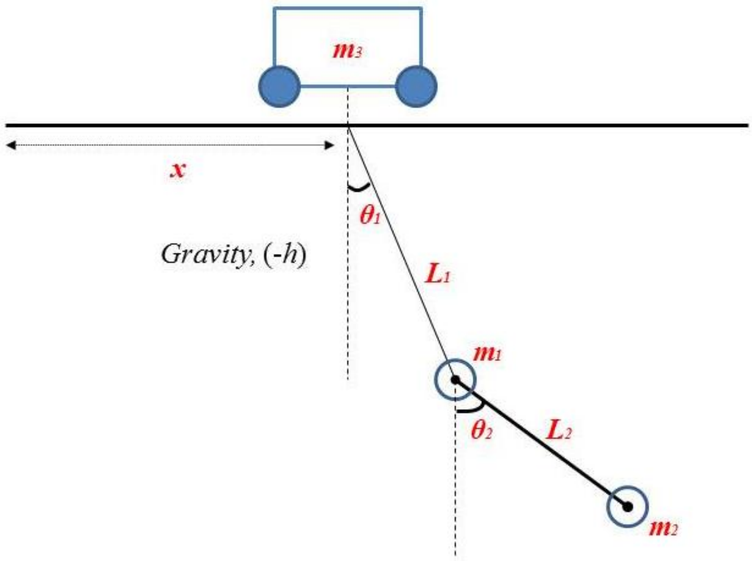

Figure 4.2: Position Analysis of DPGCS

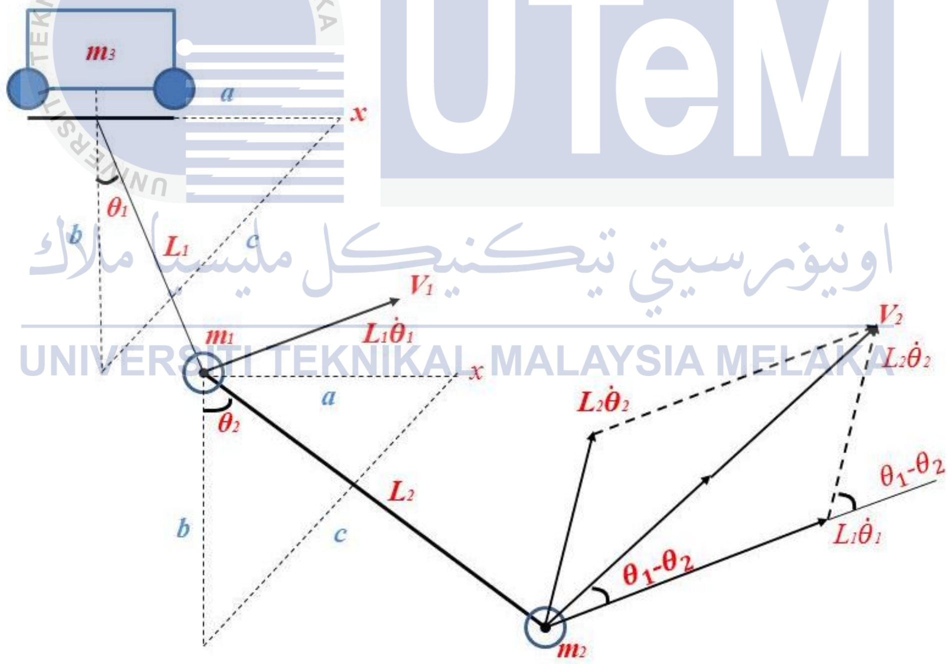

Figure 4.3: Velocity Analysis

The value of V_1 can be written as:

$$V_1 = L_1 \frac{d\theta}{dt}$$

$$= L_1 \dot{\theta}_1 \qquad (4.3)$$

$$V_1{}^2 = \left(L_1 \dot{\theta}_1\right)^2 \qquad (4.3.1)$$

By using the cosine formula, V_2 can be written as:

$$c^2 = a^2 + b^2 - 2ab\cos\theta \qquad (4.4)$$

$$V_2{}^2 = \left(L_1 \dot{\theta}_1\right)^2 + \left(L_2 \dot{\theta}_2\right)^2 - 2\left(L_1 \dot{\theta}_1\right)\left(L_2 \dot{\theta}_2\right)\cos(\theta_1 - \theta_2)$$

$$= \left(L_1 \dot{\theta}_1\right)^2 + \left(L_2 \dot{\theta}_2\right)^2 + 2\, L_1 \dot{\theta}_1 L_2 \dot{\theta}_2 \cos(\theta_1 - \theta_2) \qquad (4.4.1)$$

With *T* and *V* are respectively kinetic and potential energies. Kinetic and potential energies can be derived as:

$$T(Kinetic\ energies) = \frac{1}{2} m V^2 \qquad (4.5)$$

$$T(Kinetic\ energies) = T_1 + T_2 + T_3 \qquad (4.5.1)$$

The value of T_1 can be calculate by insert the equation (4.3.1) into $V_1{}^2$,

$$T_1 = \frac{1}{2} m_1 V_1{}^2$$

$$= \frac{1}{2}m_1\left[\dot{x}^2 + \left(L_1\dot{\theta}_1\right)^2 + 2\dot{x}L_1\dot{\theta}_1\cos\theta_1\right] \tag{4.5.2}$$

The value of T_2 can be calculate by insert the equation (4.4.1) into ${V_2}^2$,

$$T_2 = \frac{1}{2}m_2\left[\dot{x}^2\left[\left(L_1\dot{\theta}_1\right)^2 + \left(L_2\dot{\theta}_2\right)^2\right] + 2\dot{x}L_1\dot{\theta}_1\cos\theta_1 + 2\dot{x}L_2\dot{\theta}_2\cos\theta_2 + 2\dot{x}L_1L_2\dot{\theta}_1\dot{\theta}_2\cos(\theta_1-\theta_2)\right] \tag{4.5.3}$$

The value of T_3 can be calculate by insert the $\dot{x}$ value into ${V_3}^2$,

$$T_3 = \frac{1}{2}m_3\dot{x}^2 \tag{4.5.4}$$

$$\therefore T = \frac{1}{2}(m_1+m_2+m_3)\dot{x}^2 + \frac{1}{2}(m_1+m_2){L_1}^2{\dot{\theta}_1}^2 + \frac{1}{2}m_2{L_2}^2{\dot{\theta}_2}^2 + (m_1+m_2)L_1\dot{\theta}_1\dot{x}\cos\theta_1 + m_2L_2\dot{\theta}_2\dot{x}\cos\theta_2 + m_2L_1L_2\dot{\theta}_1\dot{\theta}_2\cos(\theta_1-\theta_2) \tag{4.6}$$

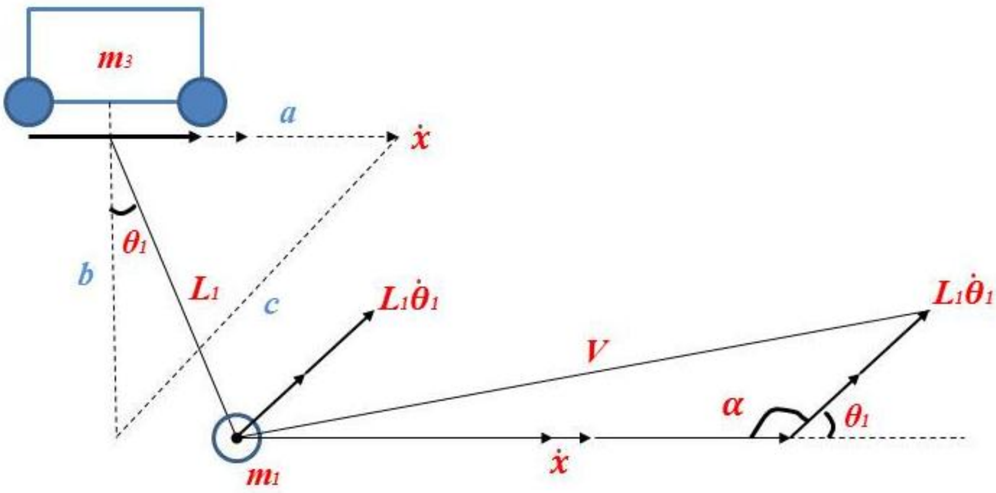

Figure 4.4: Simplify of Velocity Analysis

$$V(potential\ energies) = V_e + V_g \tag{4.7}$$

k = 0, as known that in term of DPGCS spring does not exists.

$$V(potential\ energies) = \frac{1}{2}kg^2 + mgh$$

$$= mgh \tag{4.7.1}$$

$$V = V_1 + V_2 + V_3 \tag{4.8}$$

$$V_1 = V_g \tag{4.8.1}$$

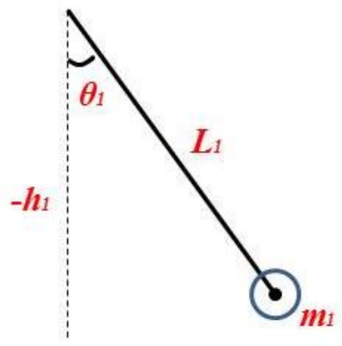

Figure 4.5: Velocity Analysis for V_1

$$h_1 = -L_1 \cos \theta_1 \tag{4.8.2}$$

$$V_1 = m_1 g h_1 \tag{4.8.3}$$

$$= m_1 g(-L_1 \cos \theta_1) \tag{4.8.4}$$

$$V_2 = V_g \tag{4.8.5}$$

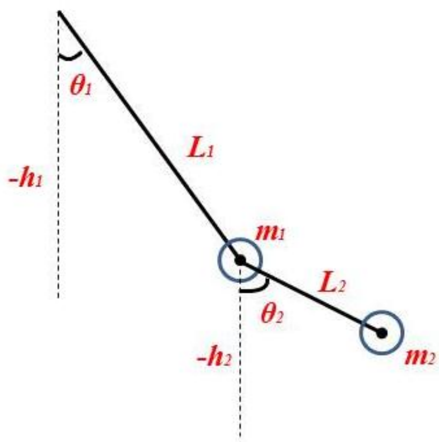

Figure 4.6: Velocity Analysis for V_2

$$h_1 = -L_1 \cos\theta_1 - L_2 \cos\theta_2 \tag{4.8.6}$$

$$V_2 = m_2 g h_2 \tag{4.8.7}$$

$$V_2 = m_2 g(-L_1 \cos\theta_1 - L_2 \cos\theta_2) \tag{4.8.8}$$

$$V_3 = V_e + V_g \tag{4.8.9}$$

$$V_3 = 0 \tag{4.8.10}$$

$$\therefore V = -(m_1 + m_2) g L_1 \cos\theta_1 - m_2 g L_2 \cos\theta_2 \tag{4.9}$$

Thus, the Lagrangian function can be obtained as:

$$L = T - V$$

$$= \frac{1}{2}(m_1 + m_2 + m_3)\dot{x}^2 + \frac{1}{2}(m_1 + m_2){L_1}^2{\dot{\theta}_1}^2 + \frac{1}{2}m_2{L_2}^2{\dot{\theta}_2}^2$$

$$+(m_1 + m_2)L_1\dot{\theta}_1\dot{x}\cos\theta_1 + m_2L_2\dot{\theta}_2\dot{x}\cos\theta_2 +$$

$$m_2L_1L_2\dot{\theta}_1\dot{\theta}_2\cos(\theta_1 - \theta_2) + (m_1 + m_2)gL_1\cos\theta_1$$

$$+m_2gL_2\cos\theta_2 \tag{4.10}$$

Solving the trolley displacement, *x* using Lagrange equations is:

$$\frac{d}{dt}\left[\frac{\partial L}{\partial \dot{x}}\right] - \frac{\partial L}{\partial x} = Q_x \tag{4.11}$$

$$\frac{\partial}{\partial x}\left(\frac{1}{2}(m_1+m_2+m_3)\dot{x}^2+\frac{1}{2}(m_1+m_2){L_1}^2{\dot{\theta}_1}^2+\frac{1}{2}m_2{L_2}^2{\dot{\theta}_2}^2\right.$$

$$+(m_1+m_2)L_1\dot{\theta}_1\dot{x}\cos\theta_1+\ m_2L_2\dot{\theta}_2\dot{x}\cos\theta_2+m_2L_1L_2\,\dot{\theta}_1\dot{\theta}_2\cos(\theta_1-\theta_2)$$

$$\left.+(m_1+m_2)gL_1\cos\theta_1+m_2gL_2\cos\theta_2\right)$$

$$\frac{\partial L}{\partial x}=0 \tag{4.11.1}$$

$$\frac{\partial}{\partial \dot{x}}\left(\frac{1}{2}(m_1+m_2+m_3)\dot{x}^2+\frac{1}{2}(m_1+m_2){L_1}^2{\dot{\theta}_1}^2+\frac{1}{2}m_2{L_2}^2{\dot{\theta}_2}^2\right.$$

$$+(m_1+m_2)L_1\dot{\theta}_1\dot{x}\cos\theta_1+\ m_2L_2\dot{\theta}_2\dot{x}\cos\theta_2+m_2L_1L_2\,\dot{\theta}_1\dot{\theta}_2\cos(\theta_1-\theta_2)$$

$$\left.+(m_1+m_2)gL_1\cos\theta_1+m_2gL_2\cos\theta_2\right)$$

$$\frac{\partial L}{\partial \dot{x}}=(m_1+m_2+m_3)\dot{x}+(m_1+m_2)L_1\dot{\theta}_1\cos\theta_1+m_2L_2\dot{\theta}_2\cos\theta_2 \tag{4.11.2}$$

$$\frac{d}{dt}\left[\frac{\partial L}{\partial \dot{x}}\right]=(m_1+m_2+m_3)\ddot{x}-(m_1+m_2)L_1{\dot{\theta}_1}^2\sin\theta_1$$

$$+(m_1+m_2)L_1\ddot{\theta}_1\cos\theta_1-m_2L_2{\dot{\theta}_2}^2\sin\theta_2+m_2L_2\ddot{\theta}_2\cos\theta_2 \tag{4.11.3}$$

$$\frac{d}{dt}\left[\frac{\partial L}{\partial \dot{x}}\right]-\frac{\partial L}{\partial x}=Q_x$$

$$\therefore\ (m_1+m_2+m_3)\ddot{x}-(m_1+m_2)L_1{\dot{\theta}_1}^2\sin\theta_1+(m_1+m_2)L_1\ddot{\theta}_1\cos\theta_1$$

$$-m_2L_2{\dot{\theta}_2}^2\sin\theta_2+\ m_2L_2\ddot{\theta}_2\cos\theta_2 \tag{4.11.4}$$

Solving the hook oscillation, θ_1 using Lagrange equations is:

$$\frac{d}{dt}\left[\frac{\partial L}{\partial \dot{\theta}_1}\right] - \frac{\partial L}{\partial \theta_1} = Q_1 \tag{4.12}$$

$$\frac{\partial}{\partial \theta_1}\Big(\frac{1}{2}(m_1+m_2+m_3)\dot{x}^2 + \frac{1}{2}(m_1+m_2){L_1}^2{\dot{\theta}_1}^2 + \frac{1}{2}m_2{L_2}^2{\dot{\theta}_2}^2$$

$$+(m_1+m_2)L_1\dot{\theta}_1\dot{x}\cos\theta_1 + m_2L_2\dot{\theta}_2\dot{x}\cos\theta_2 + m_2L_1L_2\,\dot{\theta}_1\dot{\theta}_2\cos(\theta_1-\theta_2)$$

$$+(m_1+m_2)gL_1\cos\theta_1 + m_2gL_2\cos\theta_2\Big)$$

$$\frac{\partial L}{\partial \theta_1} = -(m_1+m_2)L_1\dot{\theta}_1\dot{x}\sin\theta_1 - m_2L_1L_2\dot{\theta}_1\dot{\theta}_2\sin(\theta_1-\theta_2)$$

$$-(m_1+m_2)gL_1\sin\theta_1 \tag{4.12.1}$$

$$\frac{\partial}{\partial \dot{\theta}_1}\Big(\frac{1}{2}(m_1+m_2+m_3)\dot{x}^2 + \frac{1}{2}(m_1+m_2){L_1}^2{\dot{\theta}_1}^2 + \frac{1}{2}m_2{L_2}^2{\dot{\theta}_2}^2$$

$$+(m_1+m_2)L_1\dot{\theta}_1\dot{x}\cos\theta_1 + m_2L_2\dot{\theta}_2\dot{x}\cos\theta_2 + m_2L_1L_2\,\dot{\theta}_1\dot{\theta}_2\cos(\theta_1-\theta_2)$$

$$+(m_1+m_2)gL_1\cos\theta_1 + m_2gL_2\cos\theta_2\Big)$$

$$\frac{\partial L}{\partial \dot{\theta}_1} = (m_1+m_2){L_1}^2\dot{\theta}_1 + (m_1+m_2)L_1\dot{x}\cos\theta_1 +$$

$$m_2L_1L_2\dot{\theta}_2\cos(\theta_1-\theta_2) \tag{4.12.2}$$

$$\frac{d}{dt}\left[\frac{\partial L}{\partial \dot{\theta}_1}\right] = (m_1 + m_2){L_1}^2\ddot{\theta}_1 - (m_1 + m_2)L_1\dot{\theta}_1\dot{x}\sin\theta_1 + (m_1 + m_2)L_1\ddot{x}\cos\theta_1$$

$$-m_2L_1L_2\dot{\theta}_1{\dot{\theta}_2}^2\sin(\theta_1 - \theta_2) + m_2L_1L_2\ddot{\theta}_2\cos(\theta_1 - \theta_2)$$

(4.12.3)

$$\frac{d}{dt}\left[\frac{\partial L}{\partial \dot{\theta}_1}\right] - \frac{\partial L}{\partial \theta_1} = Q_1$$

$$\therefore (m_1 + m_2){L_1}^2\ddot{\theta}_1 - (m_1 + m_2)L_1\dot{\theta}_1\dot{x}\sin\theta_1 + (m_1 + m_2)L_1\ddot{x}\cos\theta_1$$

$$-m_2L_1L_2\dot{\theta}_1{\dot{\theta}_2}^2\sin(\theta_1 - \theta_2) + m_2L_1L_2\ddot{\theta}_2\cos(\theta_1 - \theta_2) +$$

$$(m_1 + m_2)L_1\dot{\theta}_1\dot{x}\sin\theta_1 \;+\; m_2L_1L_2\dot{\theta}_1\dot{\theta}_2\sin(\theta_1 - \theta_2)$$

$$+(m_1 + m_2)gL_1\sin\theta_1 = 0 \tag{4.12.4}$$

Solving the hook oscillation, θ_2 using Lagrange equations is:

$$\frac{d}{dt}\left[\frac{\partial L}{\partial \dot{\theta}_2}\right] - \frac{\partial L}{\partial \theta_2} = Q_2 \tag{4.13}$$

$$\frac{\partial}{\partial \theta_2}\left(\frac{1}{2}(m_1 + m_2 + m_3)\dot{x}^2 + \frac{1}{2}(m_1 + m_2){L_1}^2{\dot{\theta}_1}^2 + \frac{1}{2}m_2{L_2}^2{\dot{\theta}_2}^2\right.$$

$$+(m_1 + m_2)L_1\dot{\theta}_1\dot{x}\cos\theta_1 + \; m_2L_2\dot{\theta}_2\dot{x}\cos\theta_2 + m_2L_1L_2\,\dot{\theta}_1\dot{\theta}_2\cos(\theta_1 - \theta_2)$$

$$\left.+(m_1 + m_2)gL_1\cos\theta_1 + m_2gL_2\cos\theta_2\right)$$

$$\frac{\partial L}{\partial \theta_2} = -\,m_2L_2\dot{\theta}_2\dot{x}\sin\theta_2 + m_2L_1L_2\dot{\theta}_1\dot{\theta}_2\sin(\theta_1 - \theta_2) - m_2gL_2\sin\theta_2$$

(4.13.1)

$$\frac{\partial}{\partial \dot{\theta}_2}\Big(\frac{1}{2}(m_1+m_2+m_3)\dot{x}^2+\frac{1}{2}(m_1+m_2)L_1{}^2\dot{\theta}_1{}^2+\frac{1}{2}m_2L_2{}^2\dot{\theta}_2{}^2$$

$$+(m_1+m_2)L_1\dot{\theta}_1\dot{x}\cos\theta_1+\ m_2L_2\dot{\theta}_2\dot{x}\cos\theta_2+m_2L_1L_2\,\dot{\theta}_1\dot{\theta}_2\cos(\theta_1-\theta_2)$$

$$+(m_1+m_2)gL_1\cos\theta_1+m_2gL_2\cos\theta_2\Big)$$

$$\frac{\partial L}{\partial \dot{\theta}_2}=m_2L_2{}^2\dot{\theta}_2+m_2L_2\dot{x}\cos\theta_2+m_2L_1L_2\dot{\theta}_1\cos(\theta_1-\theta_2) \qquad (4.13.2)$$

$$\frac{d}{dt}\left[\frac{\partial L}{\partial \dot{\theta}_2}\right]=m_2L_2{}^2\ddot{\theta}_1-m_2L_2\dot{\theta}_2\dot{x}\sin\theta_2+m_2L_2\ddot{x}\cos\theta_2+$$

$$m_2L_1L_2\dot{\theta}_1{}^2\dot{\theta}_2\sin(\theta_1-\theta_2)+\ m_2L_1L_2\ddot{\theta}_1\cos(\theta_1-\theta_2) \qquad (4.13.3)$$

$$\frac{d}{dt}\left[\frac{\partial L}{\partial \dot{\theta}_2}\right]-\frac{\partial L}{\partial \theta_2}=Q_2$$

$$\therefore m_2L_2{}^2\ddot{\theta}_2-m_2L_2\dot{\theta}_2\dot{x}\sin\theta_2+m_2L_2\ddot{x}\cos\theta_2+m_2L_1L_2\dot{\theta}_1{}^2\dot{\theta}_2\sin(\theta_1-\theta_2)$$

$$+m_2L_1L_2\ddot{\theta}_1\cos(\theta_1-\theta_2)+m_2L_2\dot{\theta}_2\dot{x}\sin\theta_2-m_2L_1L_2\dot{\theta}_1\dot{\theta}_2\sin(\theta_1-\theta_2)$$

$$+\ m_2gL_2\sin\theta_2=0 \qquad (4.13.4)$$

From (4.11.4), (4.12.4) and (4.13.4), a set of three equations is obtained that:

$$\frac{d}{dt}\left[\frac{\partial L}{\partial \dot{x}}\right]-\frac{\partial L}{\partial x}=F \qquad \frac{d}{dt}\left[\frac{\partial L}{\partial \dot{\theta}_1}\right]-\frac{\partial L}{\partial \theta_1}=0 \qquad \frac{d}{dt}\left[\frac{\partial L}{\partial \dot{\theta}_2}\right]-\frac{\partial L}{\partial \theta_2}=0$$

Matrices $M(q) \in \Re^{3x3}, C(q,\dot{q}) \in \Re^{3x3}$and $\mathrm{G}(q) \in \Re^{3}$ are representing the inertia, Centrifugal-Coriolis and gravity. For simple analysis, this term defined as:

$$\frac{d}{dt}\left[\frac{\partial L}{\partial \dot{x}}\right] - \frac{\partial L}{\partial x} = Q_x$$

$$\therefore (m_1 + m_2 + m_3)\ddot{x} - (m_1 + m_2)L_1\dot{\theta}_1^{\;2} \sin\theta_1 + (m_1 + m_2)L_1\ddot{\theta}_1 \cos\theta_1$$
$$-m_2L_2\dot{\theta}_2^{\;2} \sin\theta_2 + m_2L_2\ddot{\theta}_2 \cos\theta_2 \qquad (4.11.4)$$

$$\frac{d}{dt}\left[\frac{\partial L}{\partial \dot{\theta}_1}\right] - \frac{\partial L}{\partial \theta_1} = Q_1$$

$$\therefore (m_1 + m_2)L_1^{\;2}\ddot{\theta}_1 - (m_1 + m_2)L_1\dot{\theta}_1\dot{x} \sin\theta_1 + (m_1 + m_2)L_1\ddot{x} \cos\theta_1$$
$$- m_2L_1L_2\dot{\theta}_1\dot{\theta}_2^{\;2} \sin(\theta_1 - \theta_2) + m_2L_1L_2\ddot{\theta}_2 \cos(\theta_1 - \theta_2) +$$
$$(m_1 + m_2)L_1\dot{\theta}_1\dot{x} \sin\theta_1 + m_2L_1L_2\dot{\theta}_1\dot{\theta}_2 \sin(\theta_1 - \theta_2)$$
$$+(m_1 + m_2)gL_1 \sin\theta_1 = 0 \qquad (4.12.4)$$

$$\frac{d}{dt}\left[\frac{\partial L}{\partial \dot{\theta}_2}\right] - \frac{\partial L}{\partial \theta_2} = Q_2$$

$$\therefore m_2L_2^{\;2}\ddot{\theta}_2 - m_2L_2\dot{\theta}_2\dot{x} \sin\theta_2 + m_2L_2\ddot{x} \cos\theta_2 + m_2L_1L_2\dot{\theta}_1^{\;2}\dot{\theta}_2 \sin(\theta_1 - \theta_2)$$
$$+ m_2L_1L_2\ddot{\theta}_1 \cos(\theta_1 - \theta_2) + m_2L_2\dot{\theta}_2\dot{x} \sin\theta_2 - m_2L_1L_2\dot{\theta}_1\dot{\theta}_2 \sin(\theta_1 - \theta_2)$$
$$+ m_2gL_2 \sin\theta_2 = 0 \qquad (4.13.4)$$

The dynamic model of DPGCS can be expressed as a matrices form.

$$M(q)\ddot{q} + C(q,\dot{q})\dot{q} + G(q) = F \tag{4.14}$$

The matrices can be simply analyze as,

$$M(q) = \begin{bmatrix} m_1 + m_2 + m_3 & (m_1 + m_2)L_1 \cos\theta_1 & m_2 L_2 \cos\theta_2 \\ (m_1 + m_2)L_1 \cos\theta_1 & (m_1 + m_2){L_1}^2 & m_2 L_1 L_2 \cos(\theta_1 - \theta_2) \\ m_2 L_2 \cos\theta_2 & m_2 L_1 L_2 \cos(\theta_1 - \theta_2) & m_2 {L_2}^2 \end{bmatrix} \tag{4.15}$$

$$C(q,\dot{q}) = \begin{bmatrix} 0 & -(m_1 + m_2)L_1\dot{\theta}_1 \sin\theta_1 & -m_2 L_2 \dot{\theta}_2 \sin\theta_2 \\ 0 & 0 & m_2 L_1 L_2 \dot{\theta}_1 \sin(\theta_1 - \theta_2) \\ 0 & -m_2 L_1 L_2 \dot{\theta}_1 \sin(\theta_1 - \theta_2) & 0 \end{bmatrix} \tag{4.16}$$

$$G(q) = \begin{bmatrix} 0 & (m_1 + m_2) g L_1 \sin\theta_1 & m_2 g L_2 \sin\theta_2 \end{bmatrix} \tag{4.17}$$

After rearrange the term (4.14), can be obtained:

$$\ddot{q} = M^{-1}(-C\dot{q} - G + F) \tag{4.18}$$

CHAPTER 5

RESULTS, ANALYSIS AND DISCUSSIONS

5.0 Overview

In this chapter, the two phases of final year project need to be done. The first phase is to observe the behavior a model of DPGCS. The investigation of DPGCS characteristic has been analyzed using MATLAB and Simulink. The behavior of DPGCS is studied by increasing the load mass. The second phases are to analyze the system with studied based on four different setting parameters. In addition, discussion on the simulation results is clearly explained.

5.1 Simulation Model of DPGCS

The initial investigation has been done by consists of the input and block model as shown in Figure 5.1 and 5.2. Bang-bang input signal that has been set ±5 volts is applied as an input force. Trolley displacement, hook oscillation and payload oscillation are observed in order to analyze the performance of DPGCS. All the parameters have been set up as followed in Figure 5.3.

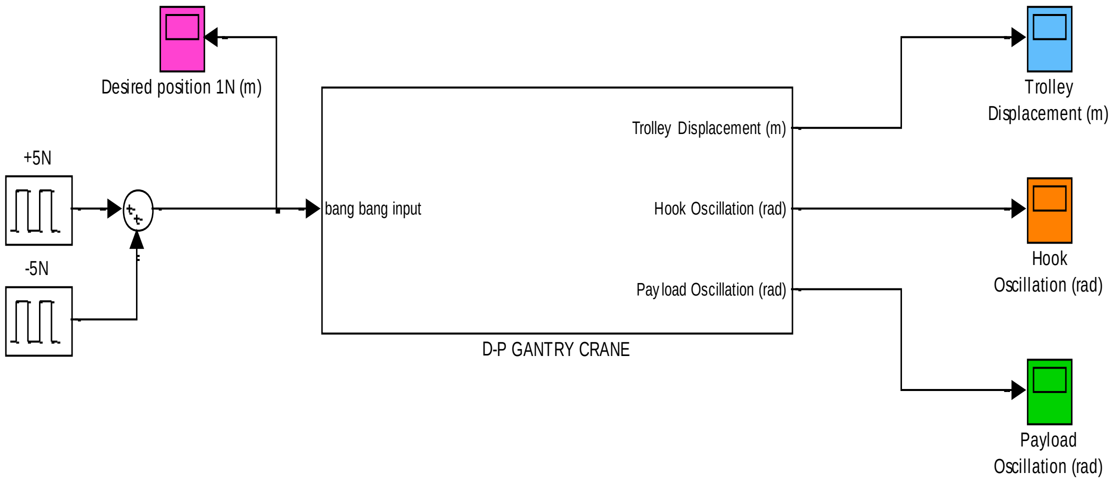

Figure 5.1: Simulink of DPGCS

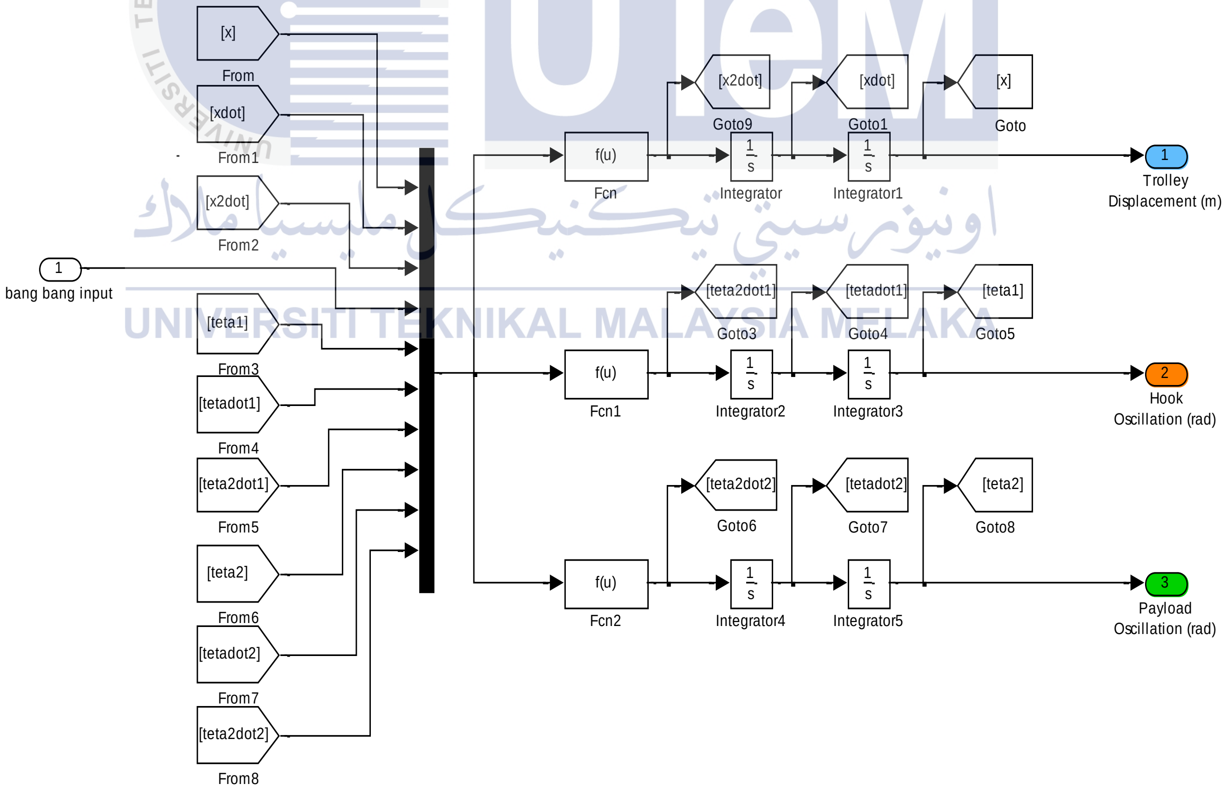

Figure 5.2: Block Diagram inside the DPGCS

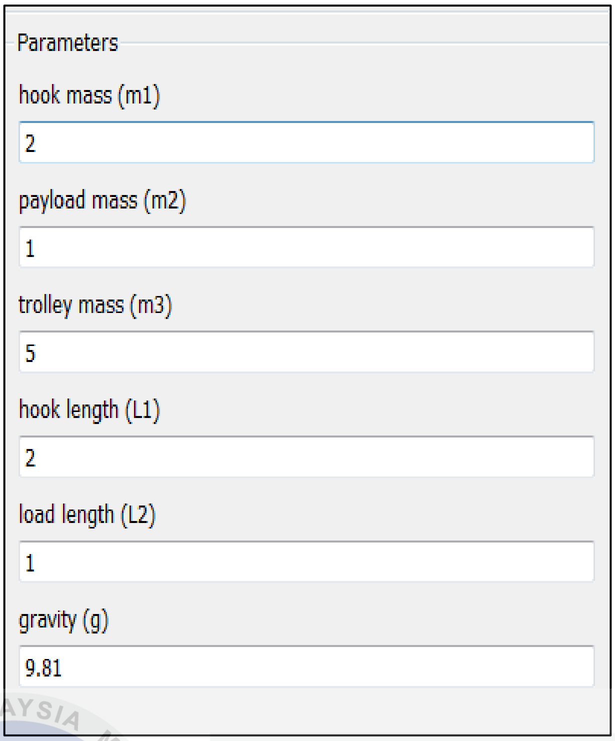

Figure 5.3: List of Parameters

5.2 First Phase: Analysis of DPGCS Behavior

To demonstrate the payload effects of the system, various payload up than 1 kg weight are simulated. Several of payloads mass is set according to the Figure 5.4. Figure 5.5 shows the desired position of 5 N input forces that has been set. While, Figure 5.6 shows the response of the system for various weight payloads. Based on the observation, it is shows that the average desired position of the trolley displacement decreases with increasing the payload weights.

5.2.1 Different Payload Mass (m_2)

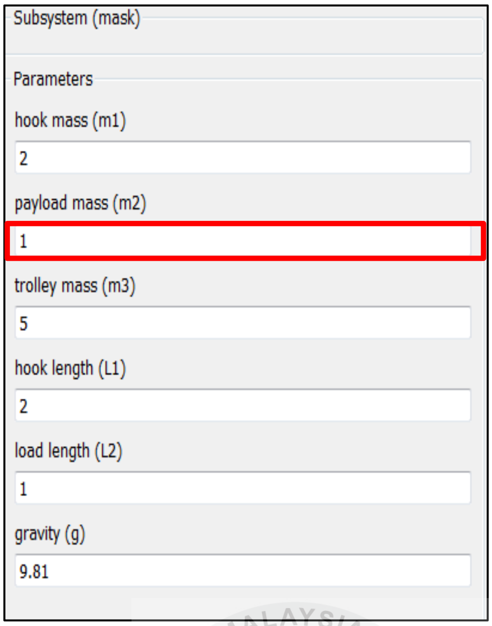

(a)

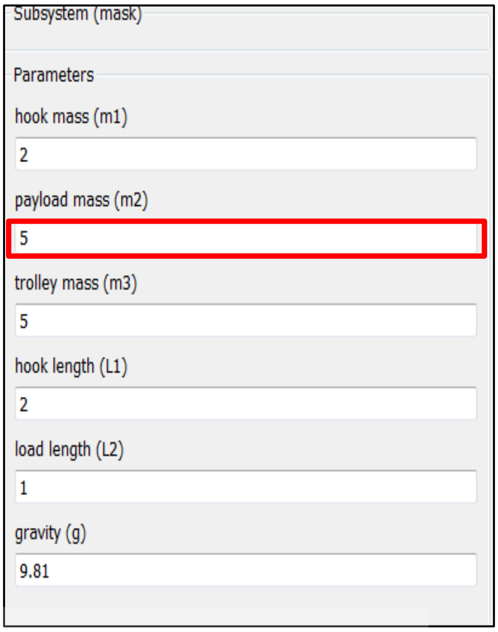

(b)

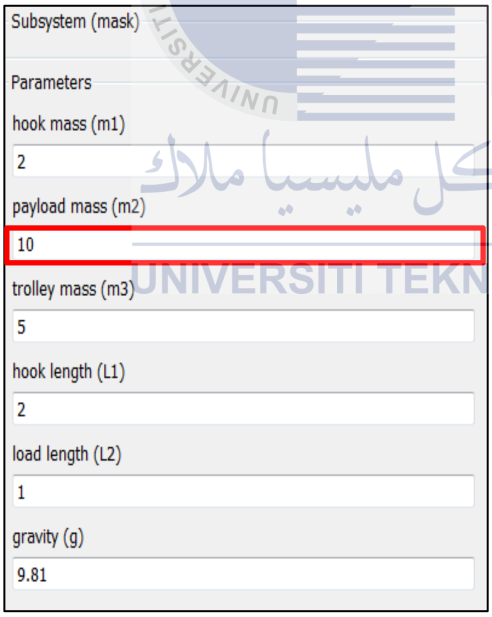

(c)

Figure 5.4: Different Payload Mass Setting:

(a) 1 kg (b) 5 kg (c) 10 kg

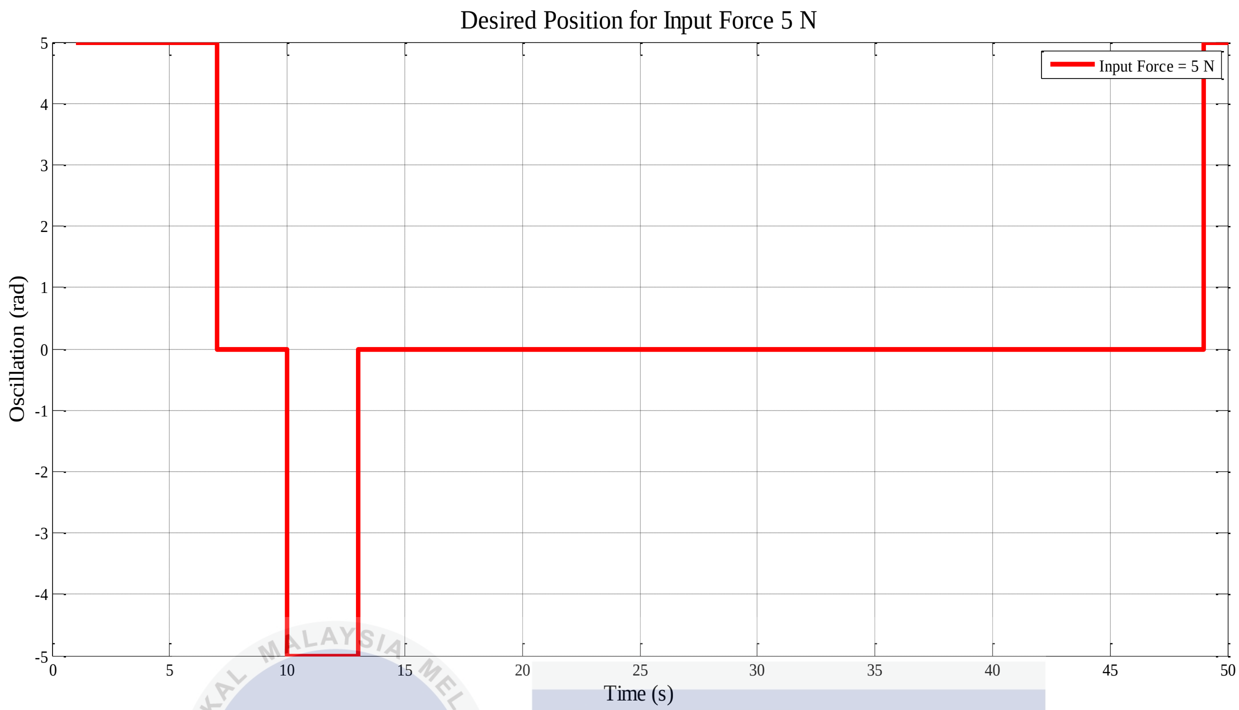

Figure 5.5: Bang-bang Input (5 N) for Different Payload Mass

Table 5.1: Trolley Displacement of with different Payload Mass (*m2*)

Payload Mass (kg)	Distance (m)
1	0.02086
5	0.1010
10	0.1234

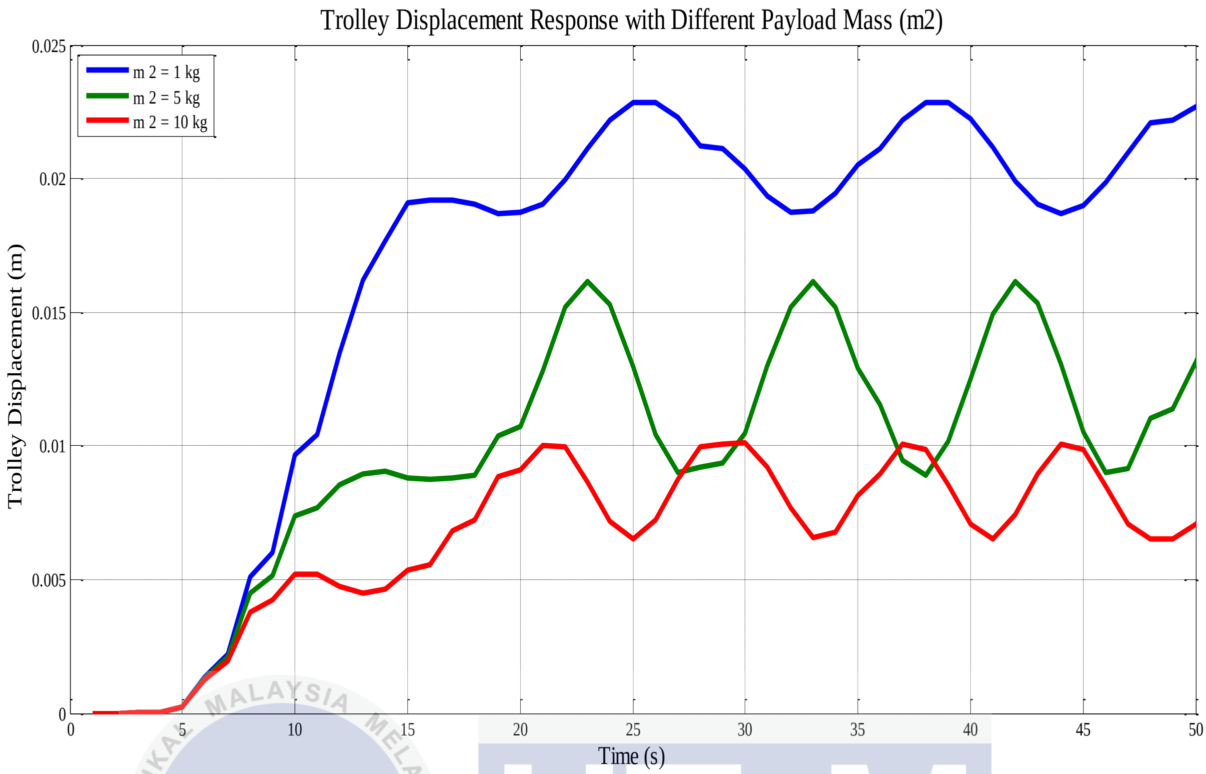

Figure 5.6: Response of the Trolley Displacement Different Payload Mass (*m2*)

The hook swing angle and the load swing angle responses can be seen in Figure 5.7 and Figure 5.8. From both figures, it is shown that the oscillations of hook swing angle and also load swing angle decrease with increasing the payload weights. Besides that, it can be seen that the responses requires more than 50 seconds to be settle down.

Table 5.2: Hook Swing Angle with Different Payload Mass (*m2*)

Payload Mass (kg)	**Maximum Hook Swing Angle (x 10^{-3} rad)**
1	0.00598
5	0.00423
10	0.00309

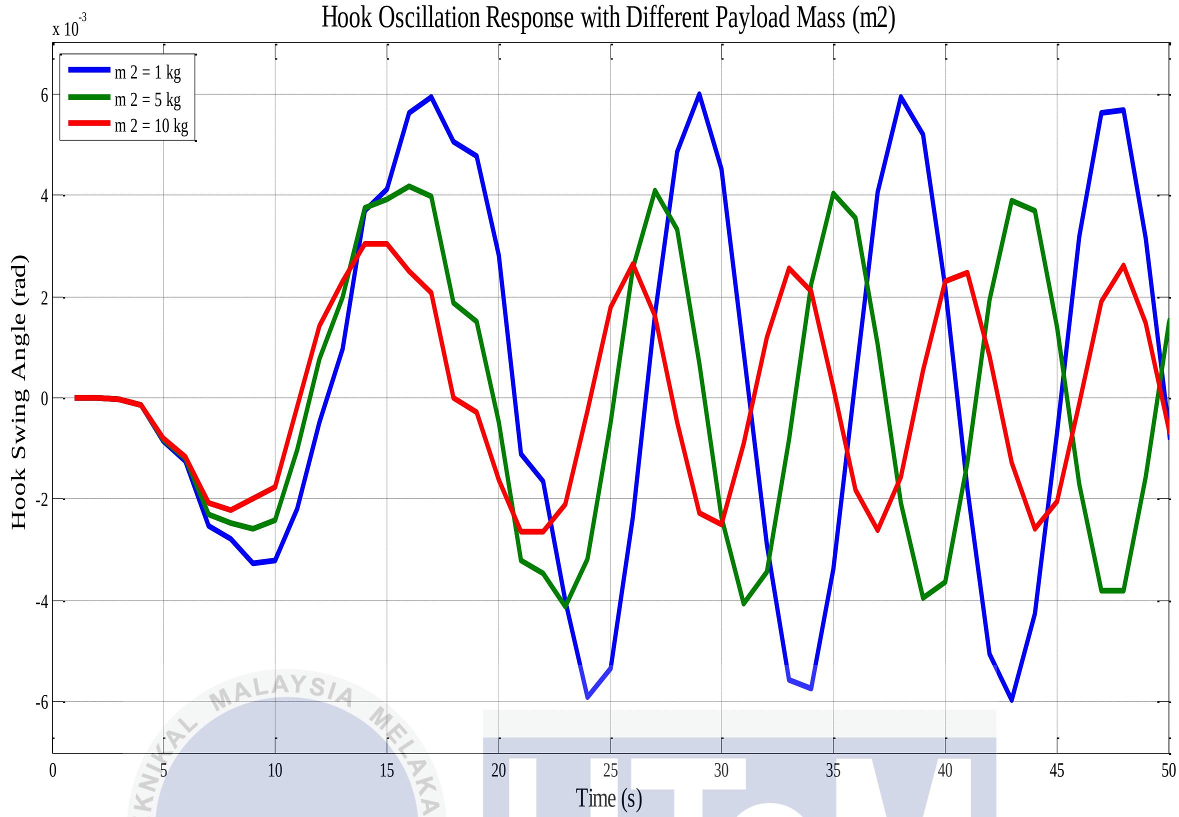

Figure 5.7: Response of Hook Swing Angle with Different Payload Mass (*m2*)

Table 5.3: Load Swing Angle with Different Payload Mass (*m2*)

Payload Mass (kg)	**Maximum Load Swing Angle (x 10^{-3} rad)**
1	0.01280
5	0.00741
10	0.00382

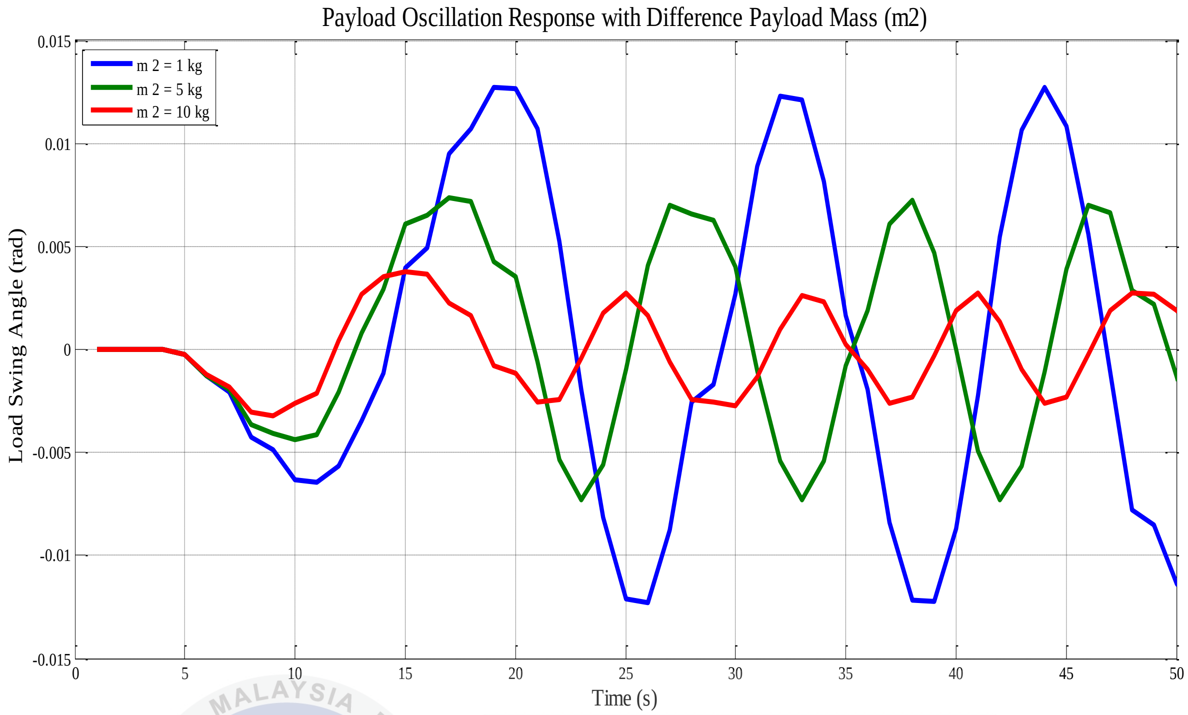

Figure 5.8: Response of Payload Swing Angle with Different Payload Mass (*m2*)

By referring the results presented in Figure 5.6, Figure 5.7 and Figure 5.8, it is conclude that the responses of the DPGCS are affected with increasing the payload weights. It also shown that, by increasing the payload mass, the oscillation of the system is decreased.

5.3 Second Phase: Analysis of DPGCS Behavior with Various Parameters Setting

For the second phase, analysis has been deeply investigated by using various system parameters of the system. The various system parameters are tested to observe the behavior of the DPGCS. System response such as trolley displacement, hook oscillation and payload oscillation are analyzed. Observation are based on various parameter includes hook and load length, input force, hook mass and trolley mass.

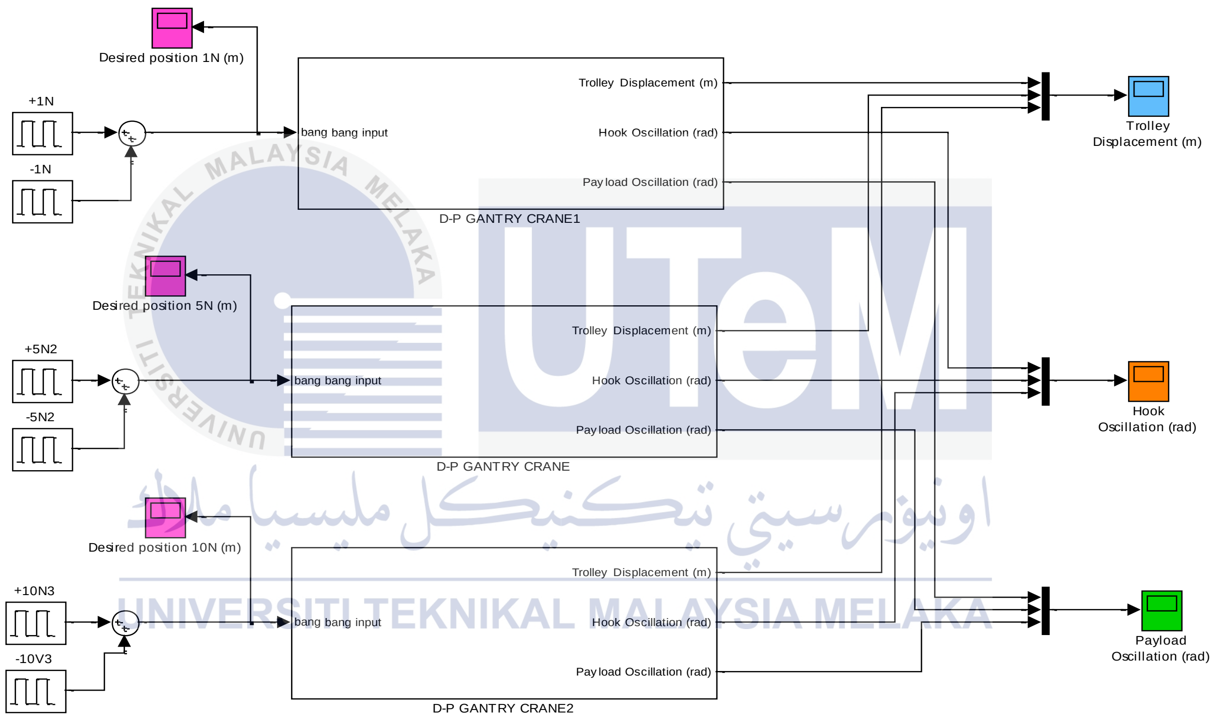

Figure 5.9: Simulink of DPGCS Model with Various Parameters Setting

5.3.1 Different Input Force (*N*)

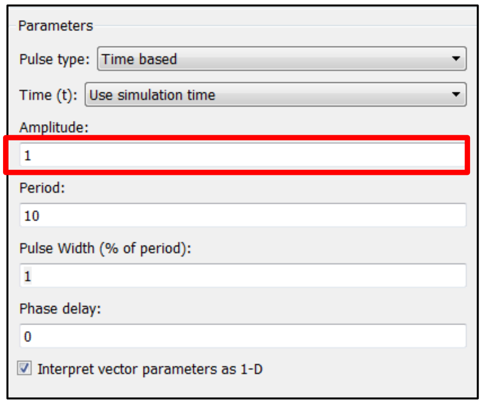

(a)

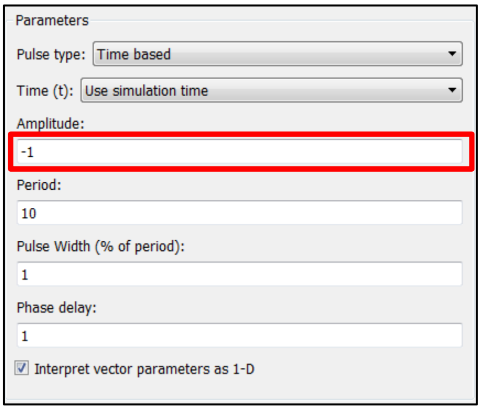

(b)

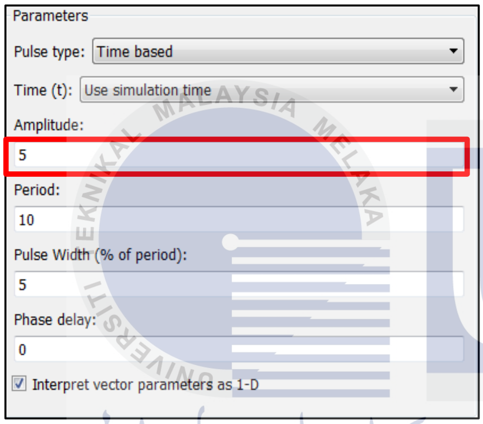

(c)

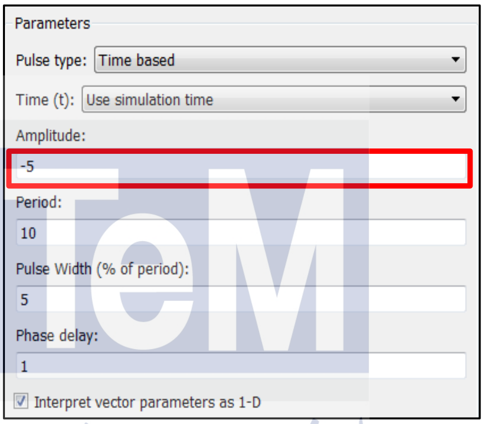

(d)

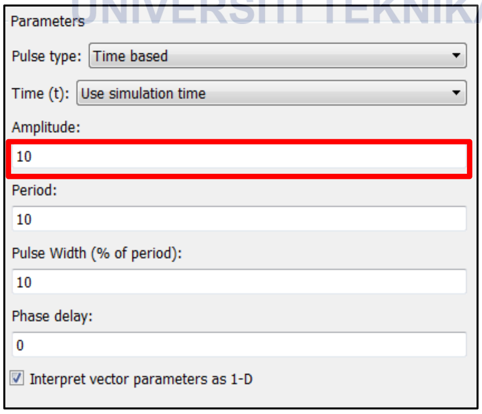

(e)

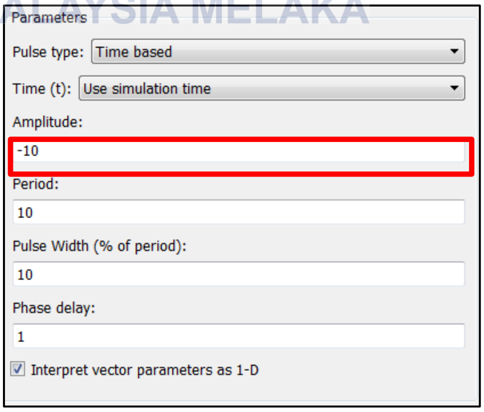

(f)

Figure 5.10: Different Input Force Setting:

(a) 1 N (b) -1 N (c) 5 N (d) -5 N (e) 10 N (f) -10 N

For the first analysis, the settings of the different input force are tested. Input force is taken into account is three times which are 1 N, 5 N and 10 N. Figure 5.11, Figure 12 and Figure 5.13, shows the desired position of various input force setting. Other parameters involved are still using the same parameters in Table 4.1. The response for trolley displacement, hook and payload oscillation is shown in Figure 5.14, Figure 5.15 and Figure 5.16 below.

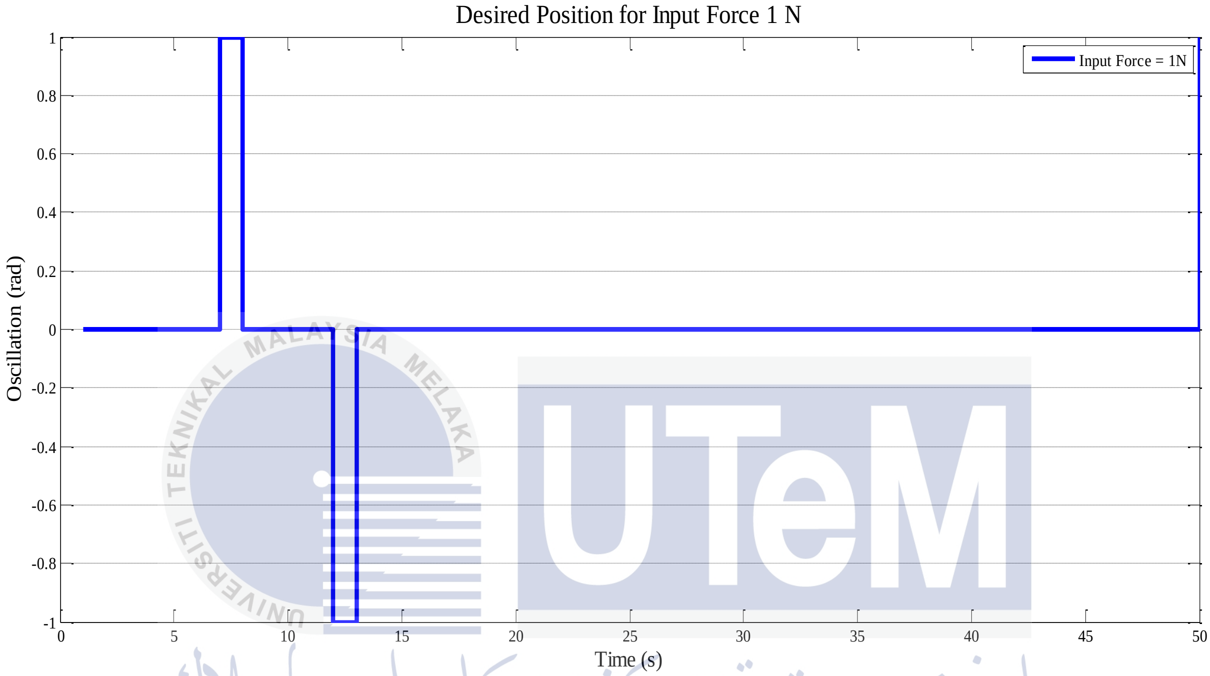

Figure 5.11: Bang-bang Input (1 N) for Different Input Force

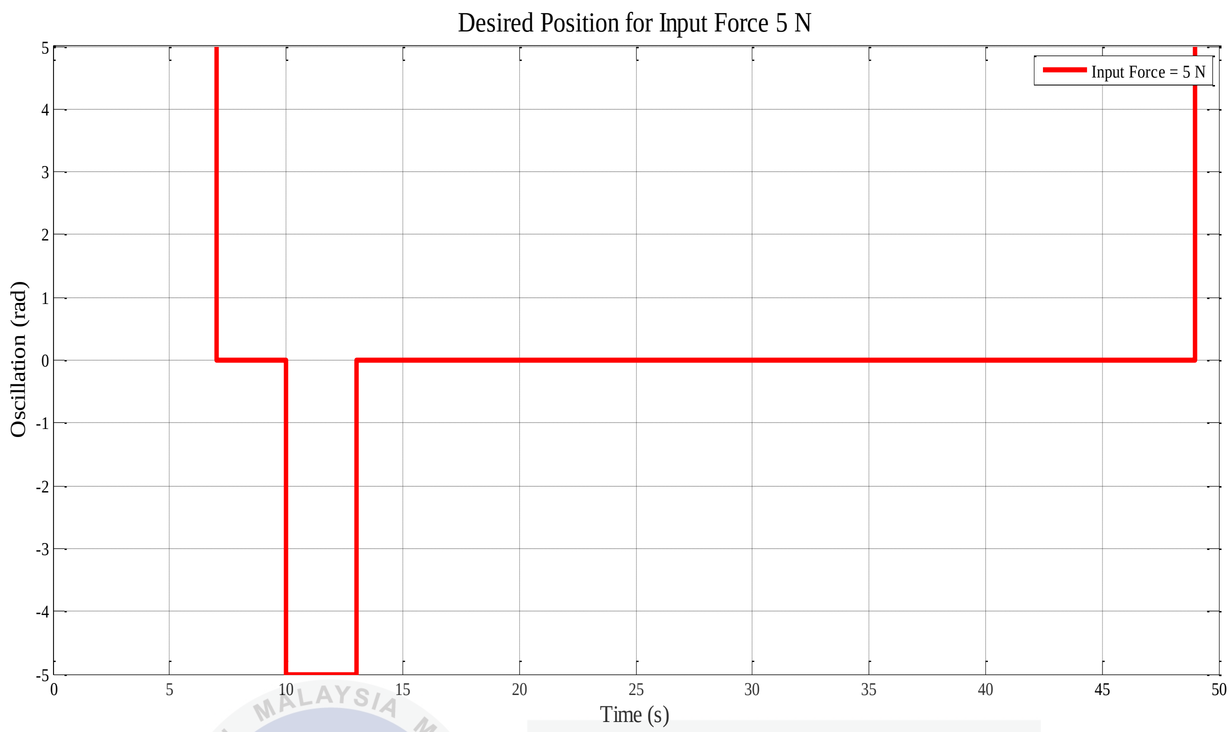

Figure 5.12: Bang-bang Input (5 N) for Different Input Force

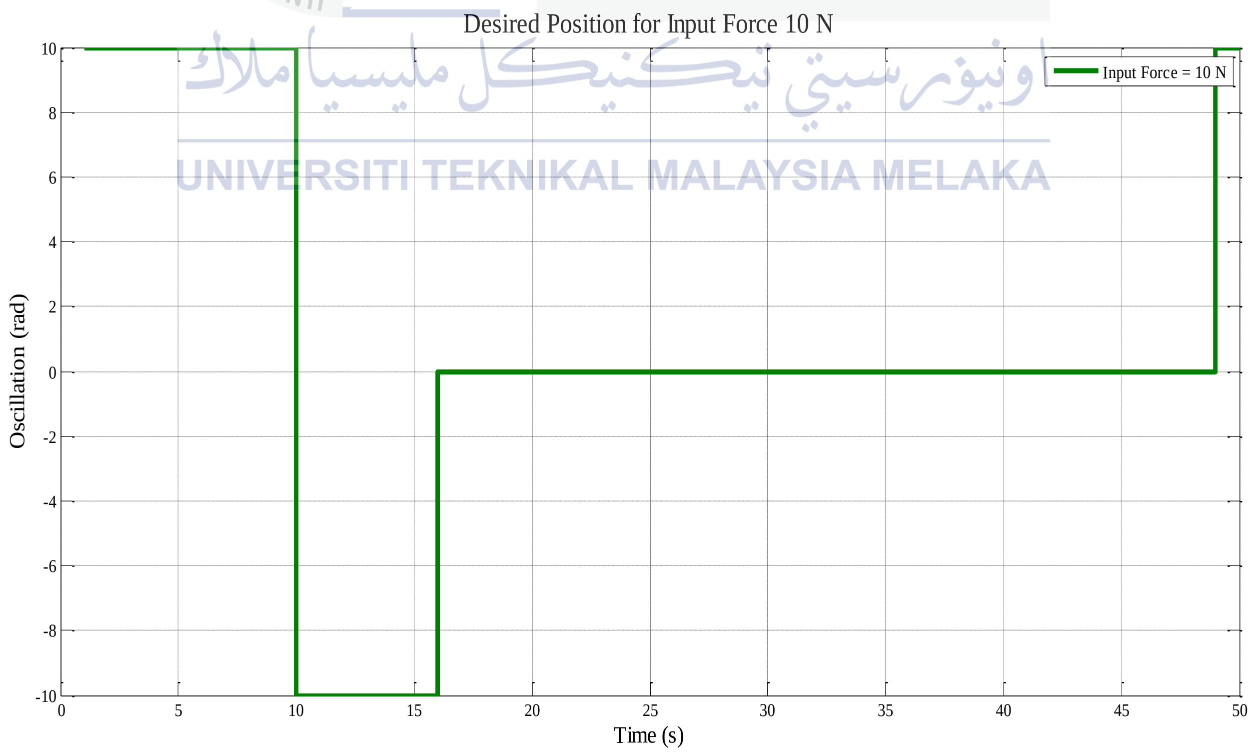

Figure 5.13: Bang-bang Input (10 N) for Different Input Force

Table 5.4: Trolley Displacement with Input Force (*N*)

Input Force (*N*)	**Distance (m)**
1	0.0009
5	0.0207
10	0.0830

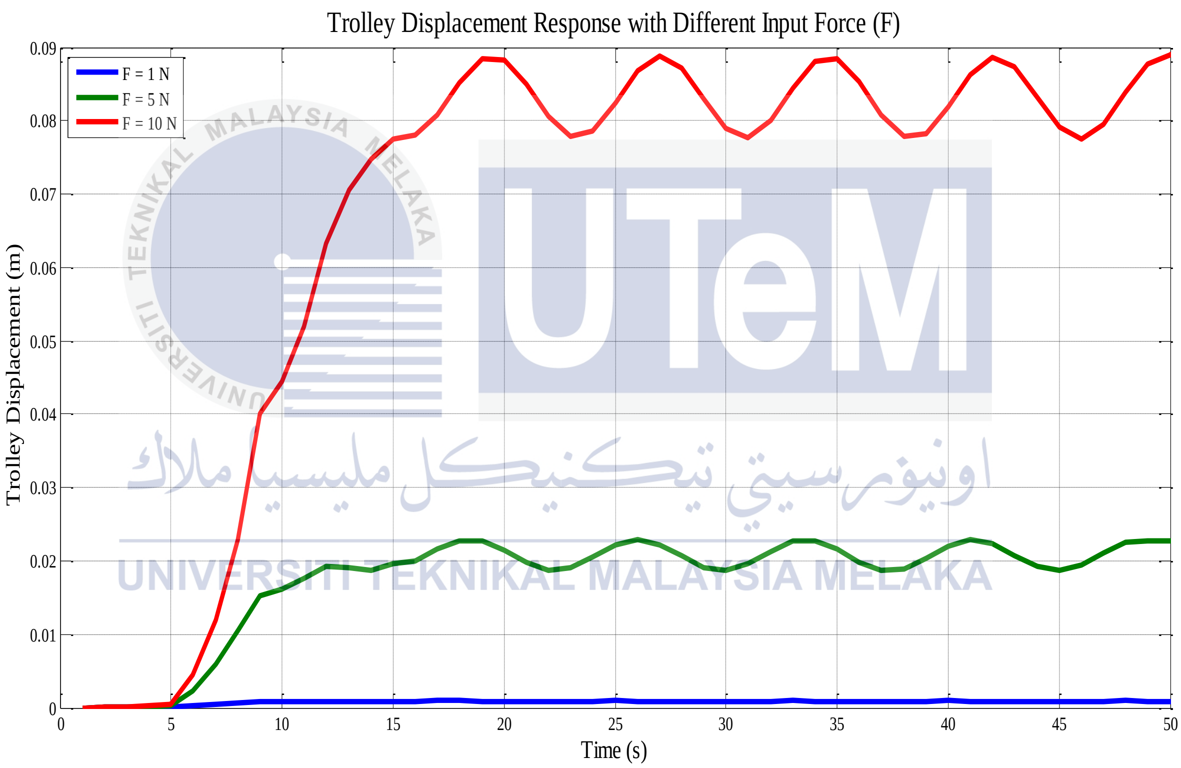

Figure 5.14: Response of Trolley Displacement with Different Input Force (*F*)

Table 5.5: Hook Swing Angle with different Input Force (*N*)

Input Force (*N*)	Maximum Hook Swing Angle (x 10^{-3} rad)
1	0.00028
5	0.00630
10	0.01500

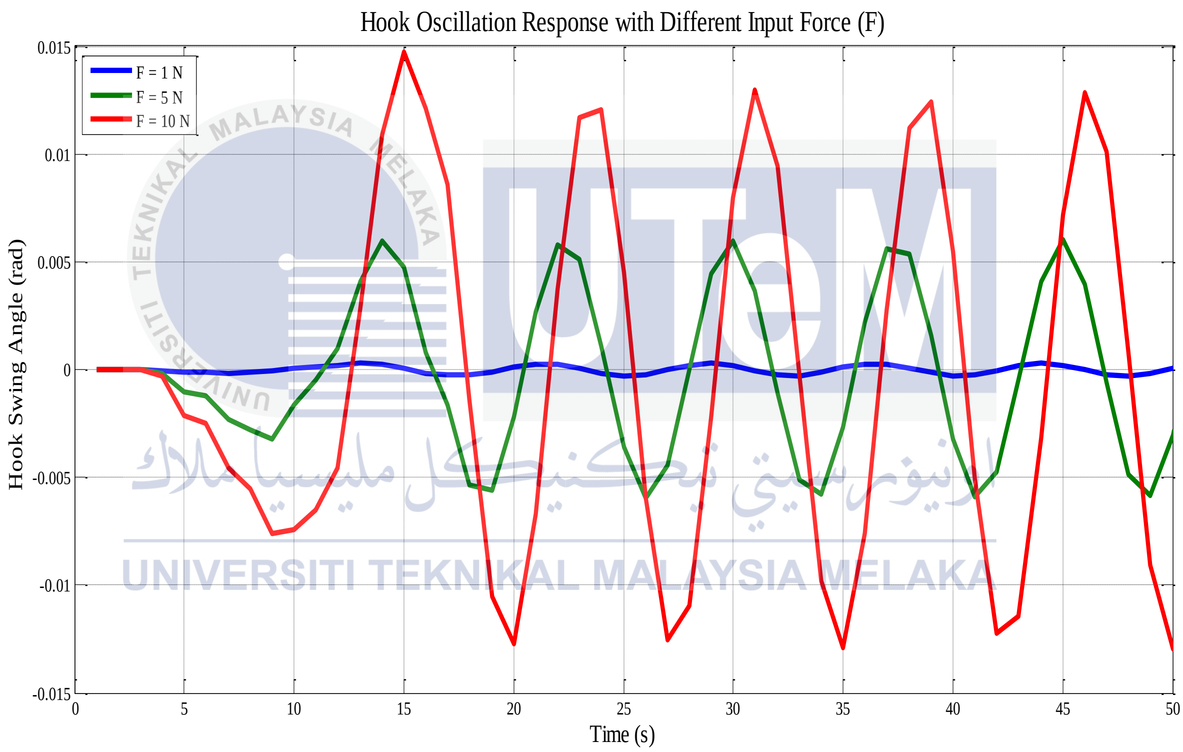

Figure 5.15: Response of Hook Swing Angle with Different Input Force (*F*).

Table 5.6: Payload Swing Angle with different Input Force (*N*)

Input Force (*N*)	**Maximum Payload Swing Angle (x 10^{-3} rad)**
1	0.00058
5	0.01275
10	0.03370

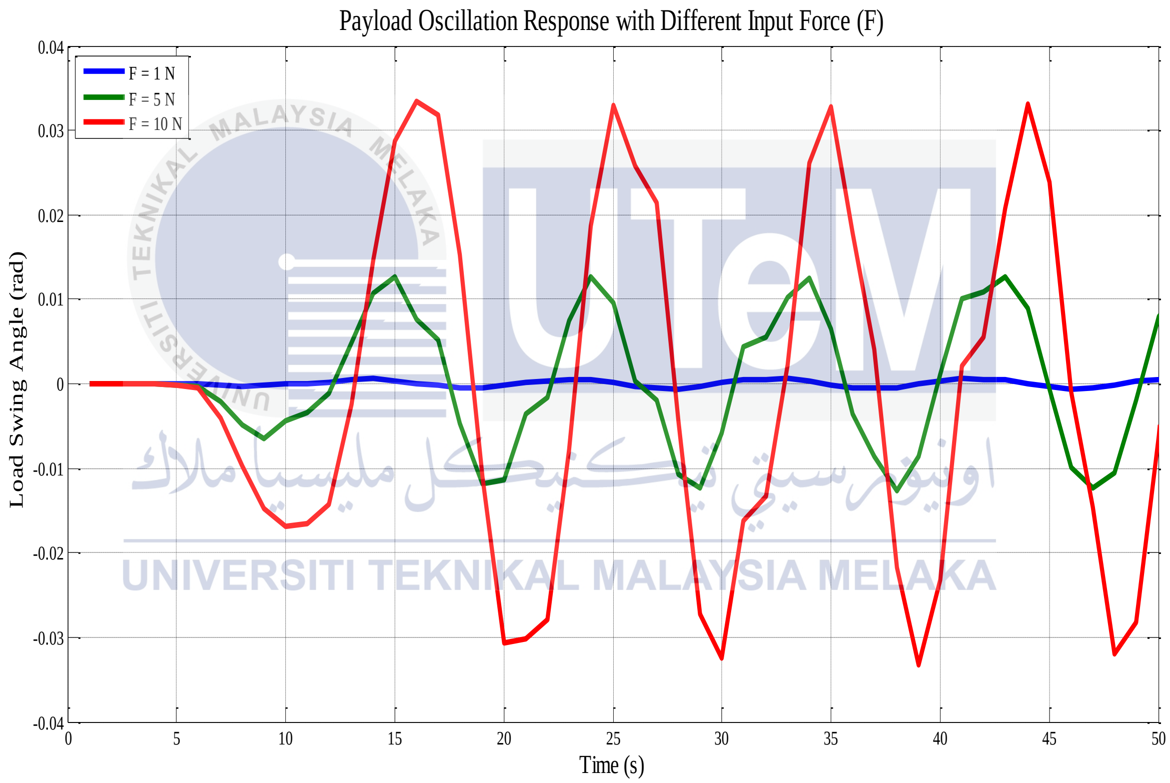

Figure 5.16: Response of Payload Swing Angle with Different Input Force (*F*).

5.3.2 Different Hook Length (L_1)

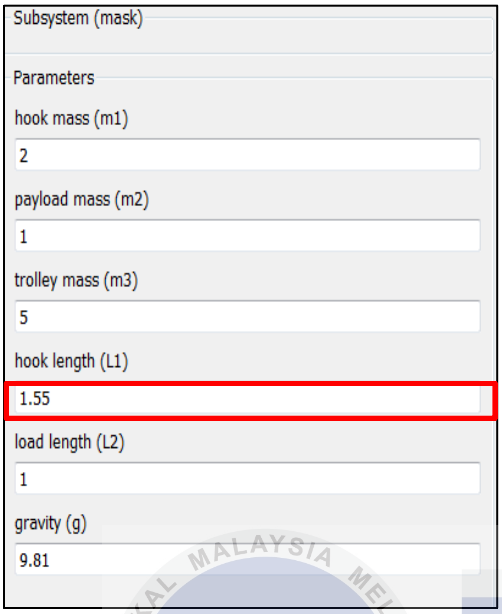

(a)

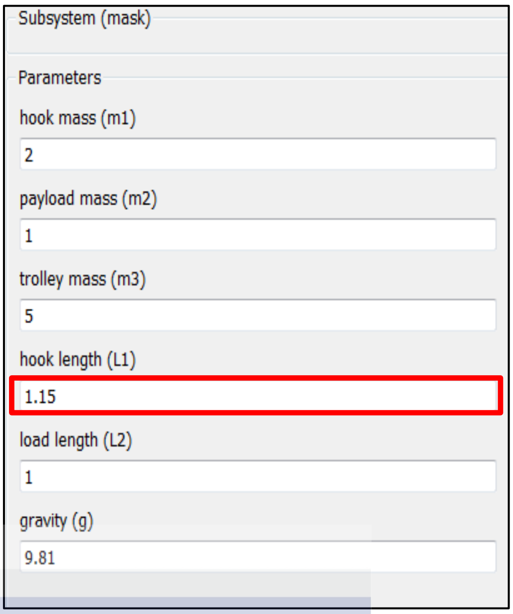

(b)

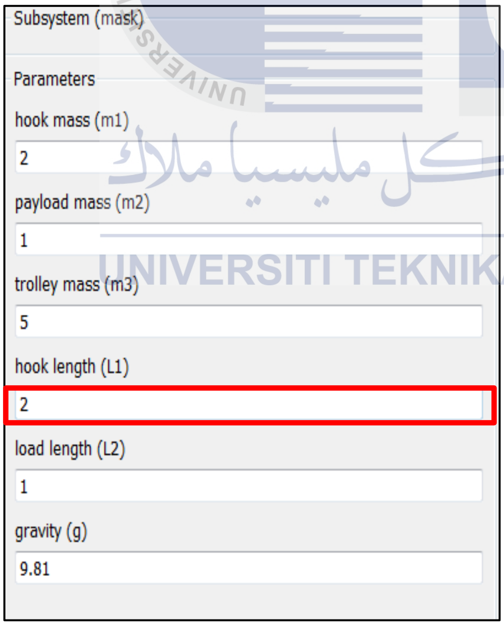

(c)

Figure 5.17: Different Hook Length Setting:

(a) 1.15 m (b) 1.55 m (c) 2.00 m

Second analysis is based on different parameters of hook length. The hook lengths are also should be tested about three times of different length which is 1.15 m, 1.55 m and 2.00 m. Figure 5.18 shows the desired position of 5 N input forces that has been set. Besides, other parameters are still using the same parameters stated in Table 4.1. The following Figure (Figure 5.19, Figure 5.20 and Figure 5.21) had shown the response of trolley displacement, hook and load oscillation.

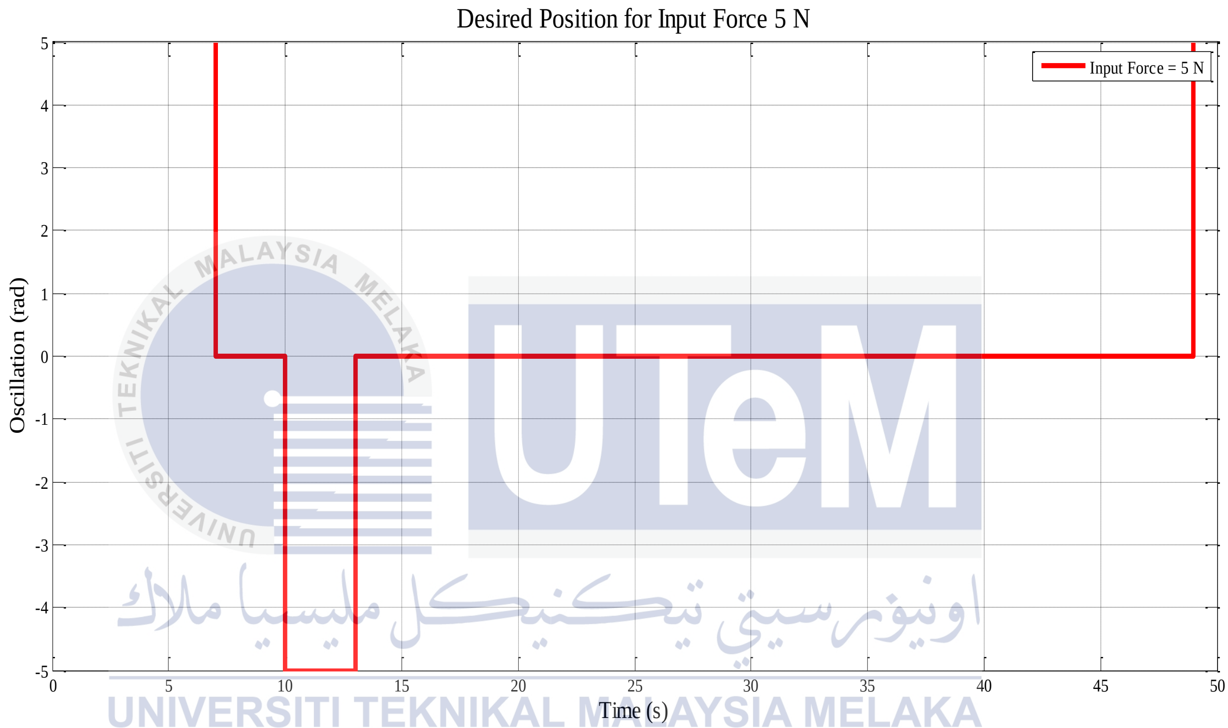

Figure 5.18: Bang-bang Input (5 N) for Different Hook Length

Table 5.7: Trolley Displacement with different Hook Length (*L1*)

Hook Length (m)	**Distance (m)**
1.15	0.01552
1.55	0.01573
2.00	0.01597

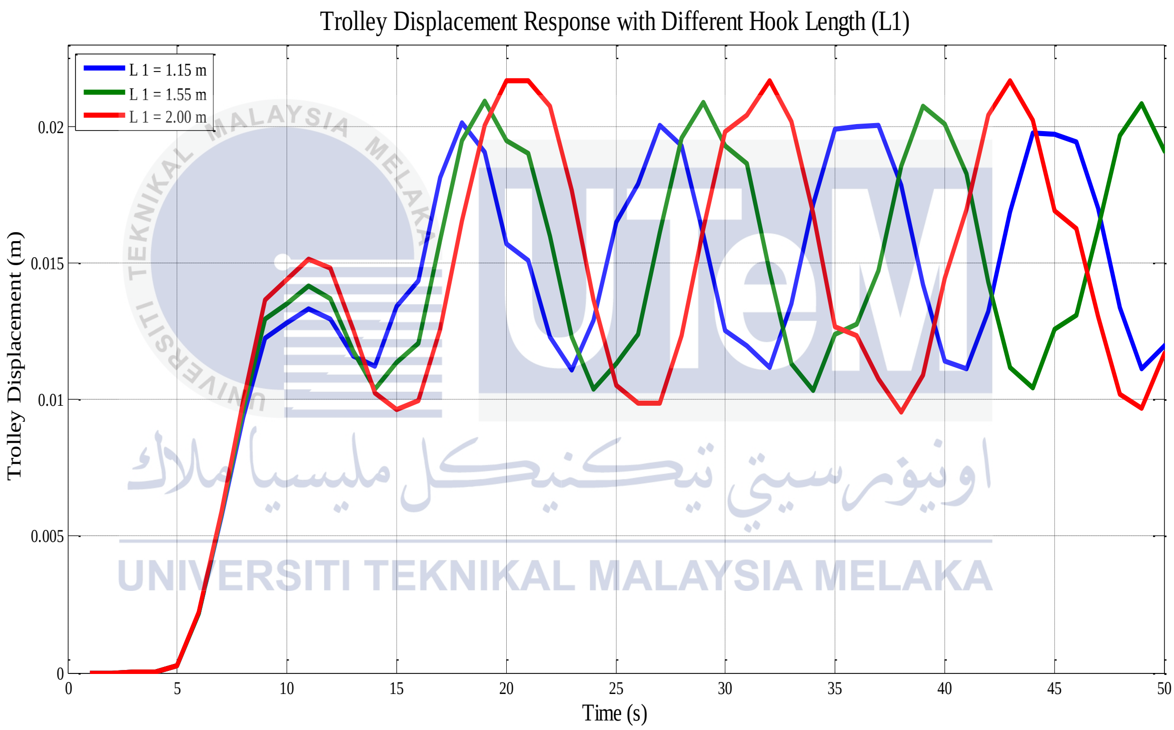

Figure 5.19: Response of Trolley Displacement with Different Hook Length (*L1*)

Table 5.8: Hook Swing Angle with different Hook Length (*L1*)

Hook Length (m)	**Maximum Hook Swing Angle (x 10^{-3} rad)**
1.15	0.00571
1.55	0.00560
2.00	0.00490

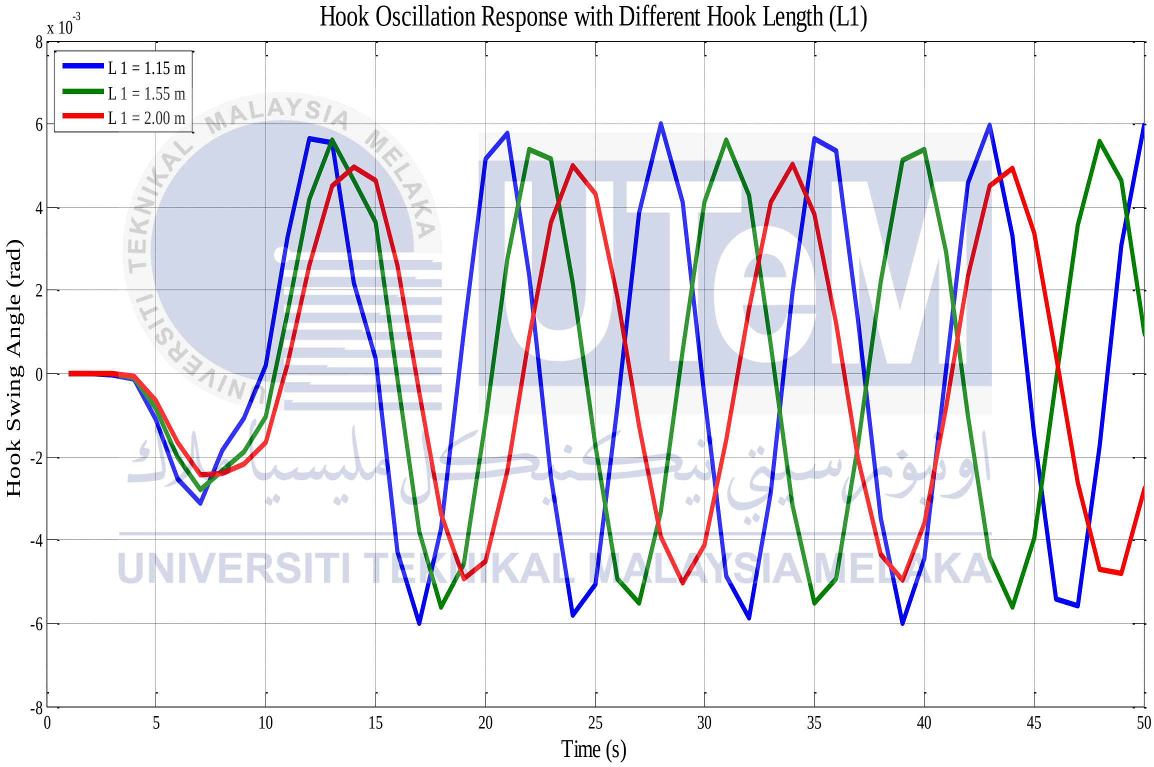

Figure 5.20: Response of Hook Swing Angle with Different Hook Length (*L1*)

Table 5.9: Payload Swing Angle with different Hook Length (*L1*)

Hook Length (m)	**Maximum Payload Swing Angle (x 10^{-3} rad)**
1.15	0.00954
1.55	0.00913
2.00	0.00810

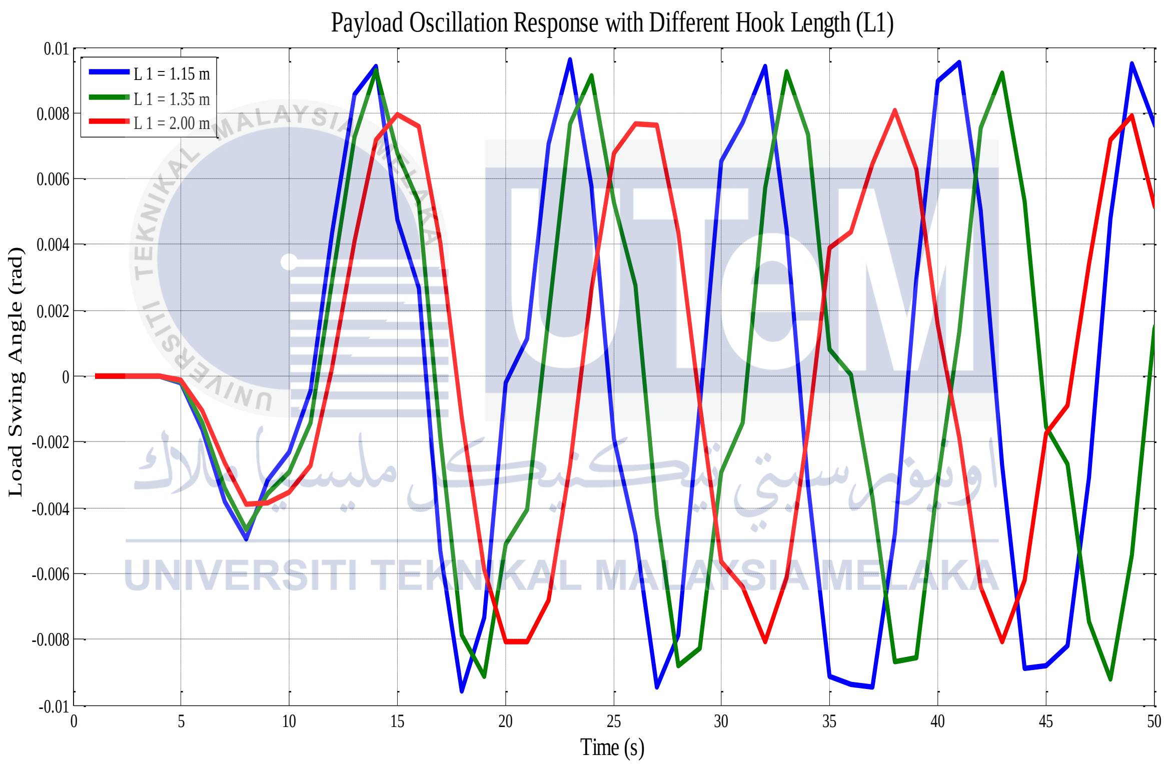

Figure 5.21: Response of Payload Swing Angle with Different Hook Length (*L1*)

5.3.3 Different Load Length (L_2)

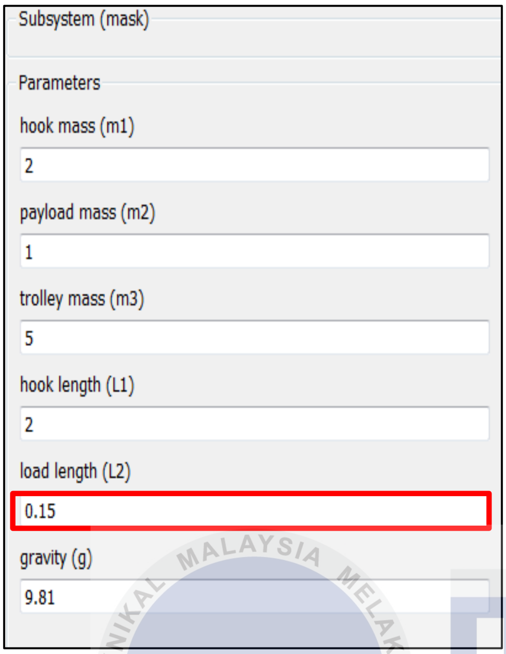

(a)

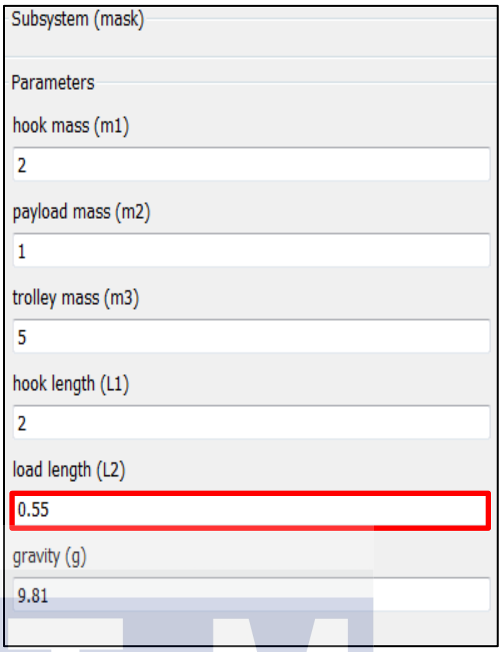

(b)

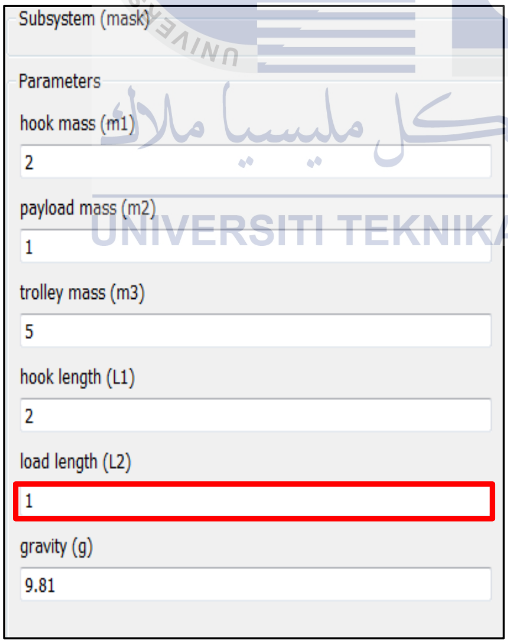

(c)

Figure 5.22: Different Load Length Setting:

(a) 0.15 m (b) 0.55 m (c) 1.00 m

For third analysis, the different length of load is tested about three times. Load lengths are tested with the value of 0.15 m, 0.55 m and 1.00 m. Figure 5.23 shows the desired position of 5 N input forces that has been set. The Figure below (Figure 5.24, Figure 5.25 and Figure 5.26) shows clearly all the response involved such as the trolley displacement, hook and load oscillation. In order to analyze the response with various parameters of load lengths, other parameters involved are using the same parameters specified in Table 4.1.

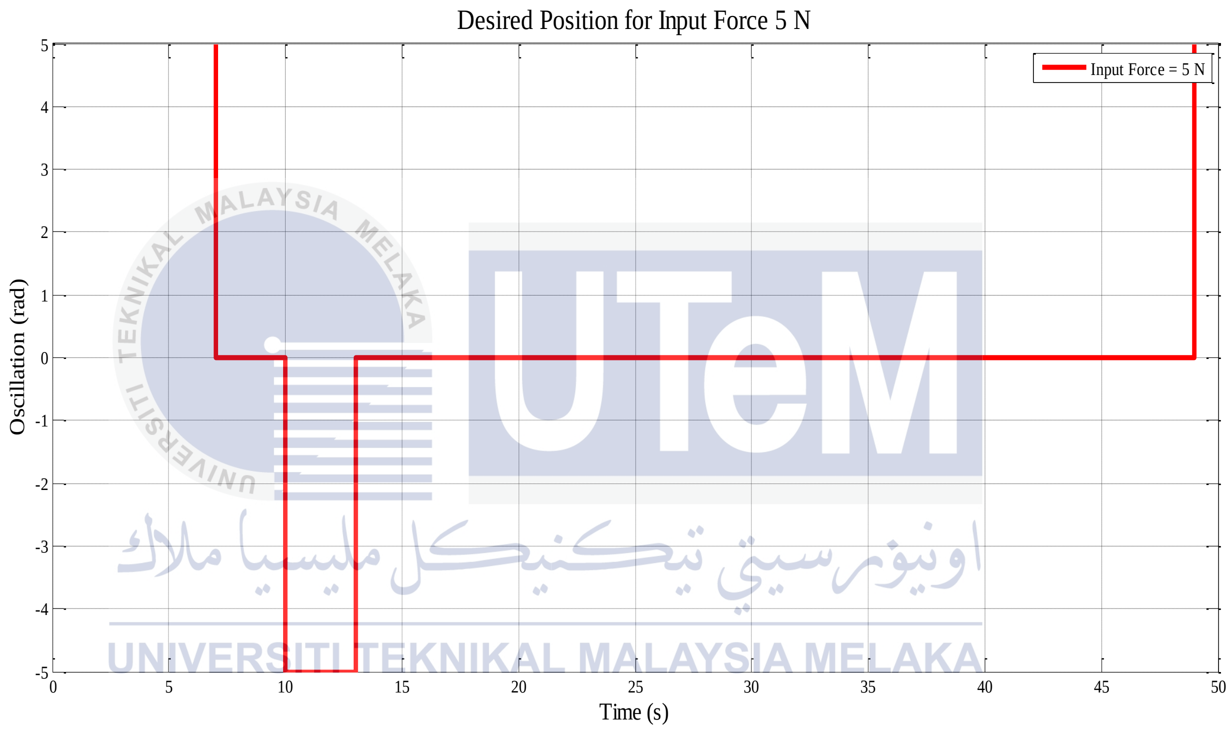

Figure 5.23: Bang-bang Input (5 N) for Different Load Length

Table 5.10: Trolley Displacement with different Load Length (*L2*)

Load Length (m)	Distance (m)
0.15	0.02082
0.55	0.02087
1.00	0.02097

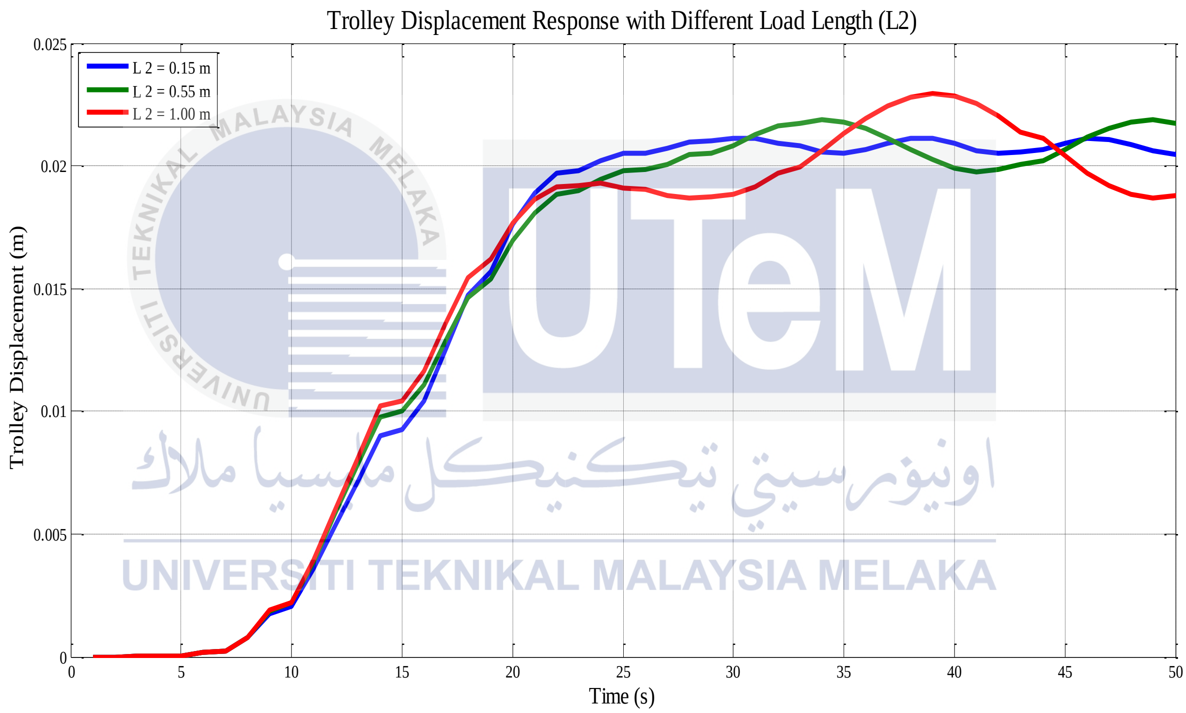

Figure 5.24: Response of Trolley Displacement with Different Load Length (*L2*)

Table 5.11: Hook Swing Angle with different Load Length (*L2*)

Load Length (m)	**Maximum Hook Swing Angle (x 10^{-3} rad)**
0.15	0.00211
0.55	0.00457
1.00	0.00610

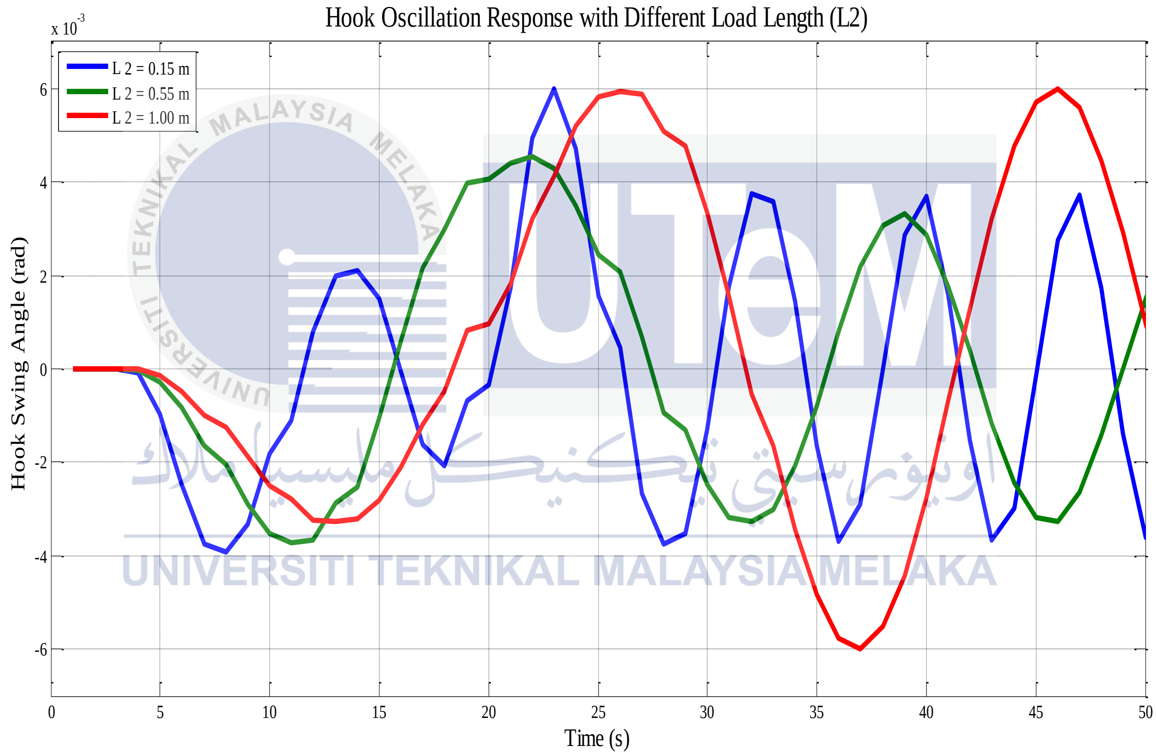

Figure 5.25: Response of Hook Swing Angle with Different Load Length (*L2*)

Table 5.12: Payload Swing Angle with different Load Length (*L2*)

Load Length (m)	Maximum Payload Swing Angle (x 10^{-3} rad)
0.15	0.00661
0.55	0.01185
1.00	0.01275

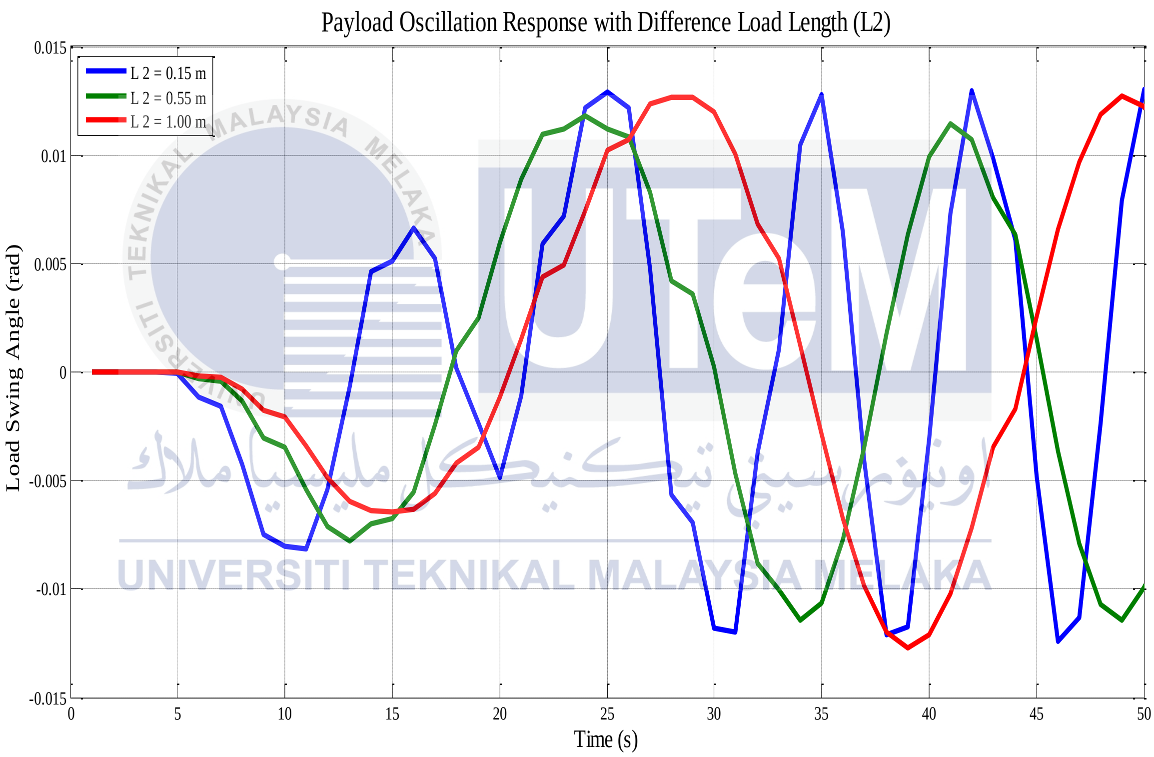

Figure 5.26: Response of Payload Swing Angle with Different Load Length (*L2*)

5.3.4 Different Hook Mass (m_1)

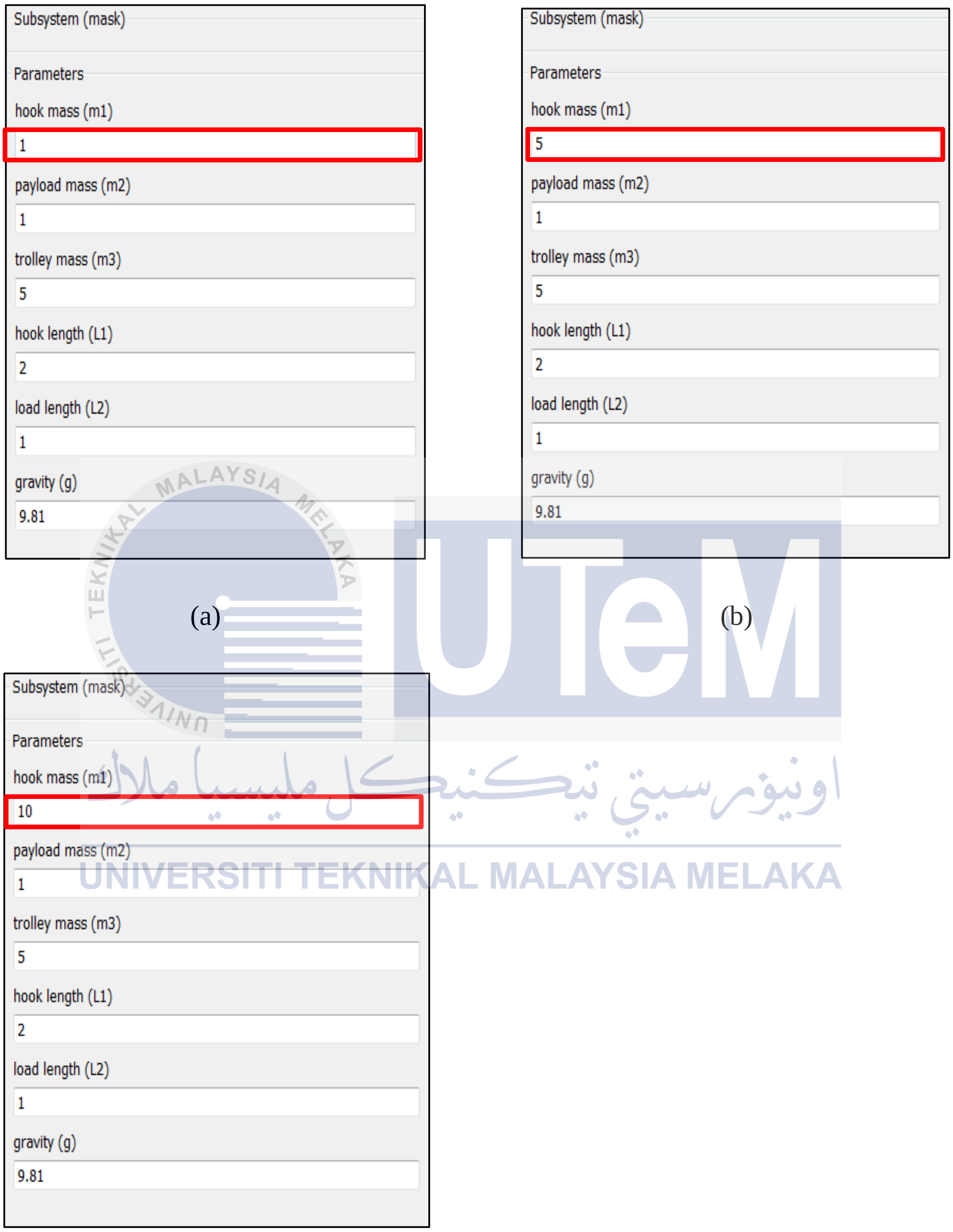

(a) (b)

(c)

Figure 5.27: Different Hook Mass Setting:

(a) 1 kg (b) 5 kg (c) 10 kg

According to Figure 5.21, there are different hook mass setting is applied into this system. The mass is taken three times by using 1 kg, 5 kg and 10 kg to show the effect of responses. Figure 5.28 shows the desired position of 5 N input forces that has been set. Besides, other parameters are still using the same parameters stated in Table 4.1. The response of for trolley displacement, hook and payload oscillation is shown in Figure 5.29, Figure 5.30 and Figure 5.31 below.

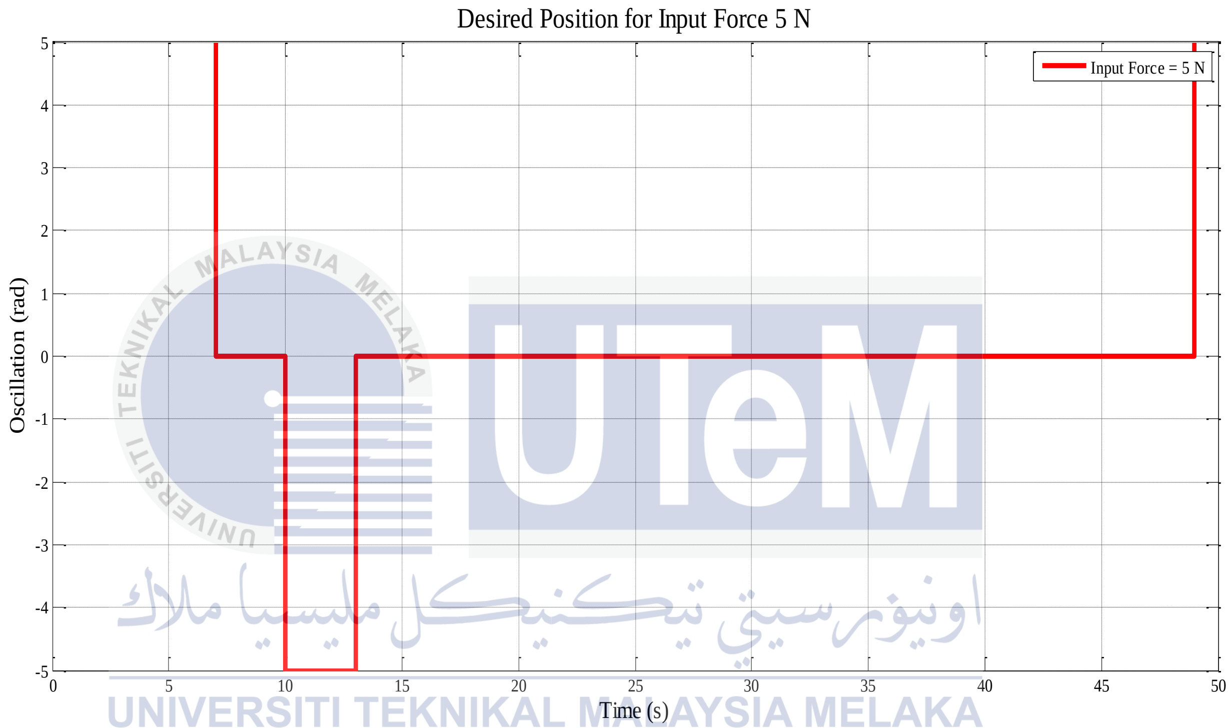

Figure 5.28: Bang-bang Input (5 N) for Different Hook Mass

Table 5.13: Trolley Displacement with different Hook Mass (*m1*)

Hook Mass (kg)	Distance (m)
1	0.01782
5	0.01144
10	0.00742

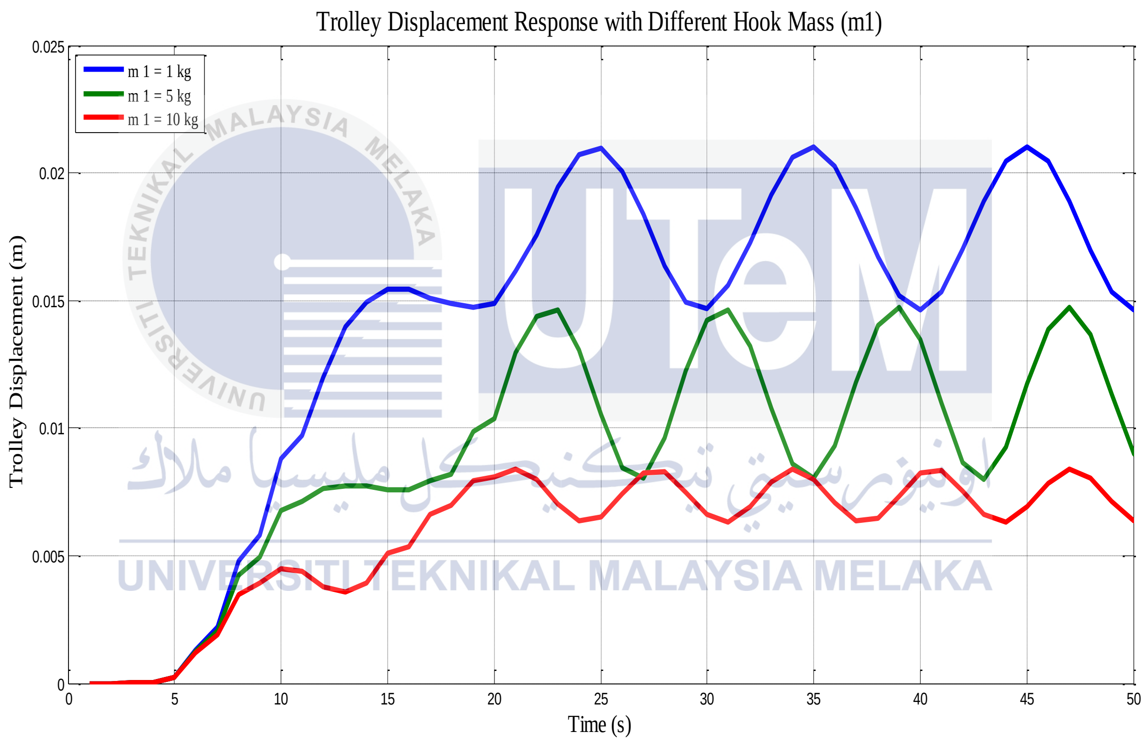

Figure 5.29: Response of Trolley Displacement with Different Hook Mass (*m1*)

Table 5.14: Hook Swing Angle with different Hook Mass (*m1*)

Hook Mass (kg)	**Maximum Hook Swing Angle (x 10^{-3} rad)**
1	0.00772
5	0.00554
10	0.00285

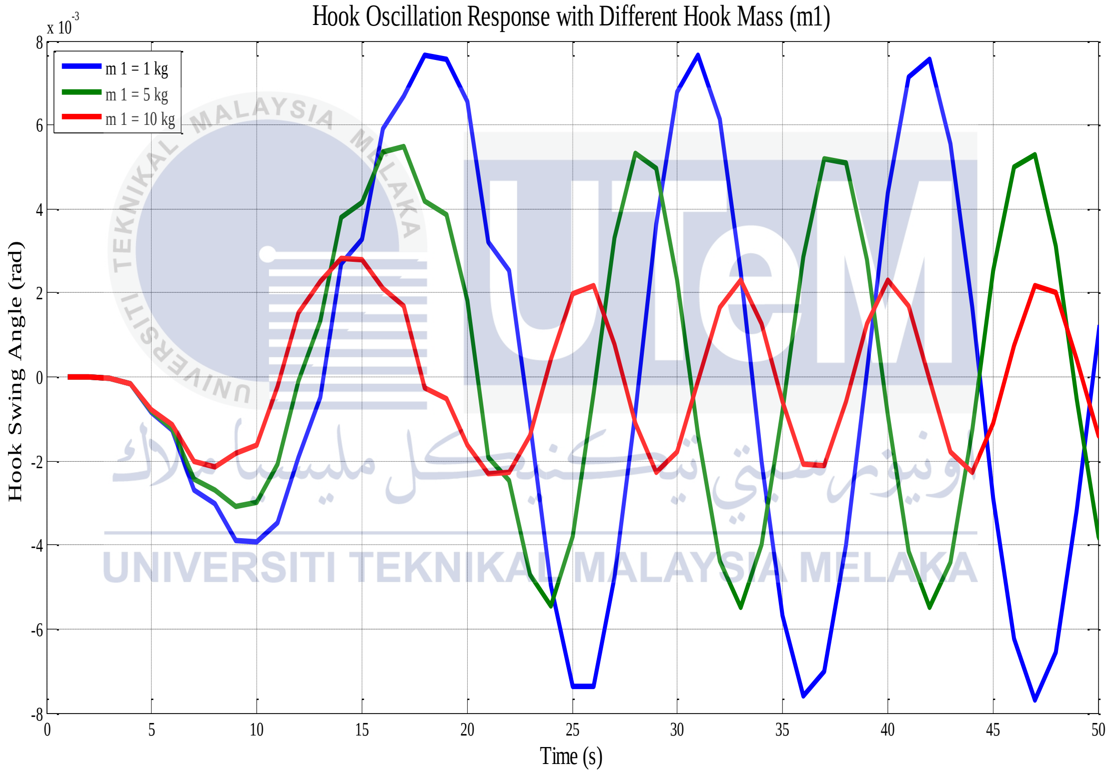

Figure 5.30: Response of Hook Oscillation with Different Hook Mass (*m1*)

Table 5.15: Payload Swing Angle with different Hook Mass (*m1*)

Hook Mass (kg)	Maximum Payload Swing Angle (x 10^{-3} rad)
1	0.01110
5	0.00499
10	0.00267

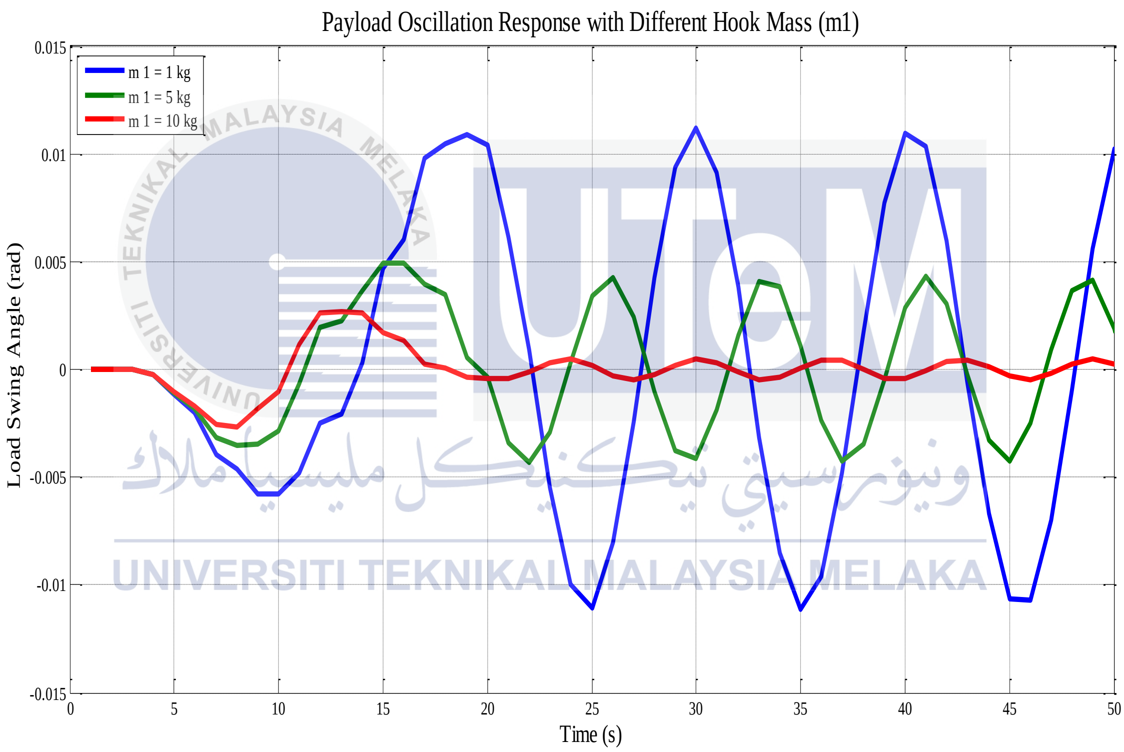

Figure 5.31: Response of Payload Oscillation with Different Hook Mass (*m1*)

5.3.5 Different Trolley Mass (m_3)

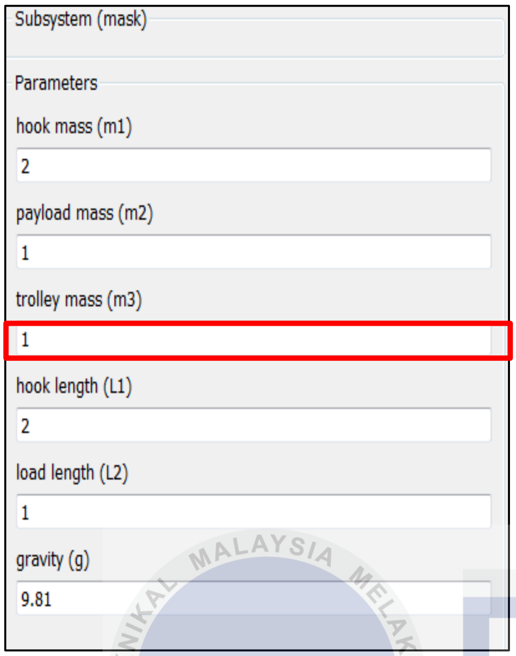

(a)

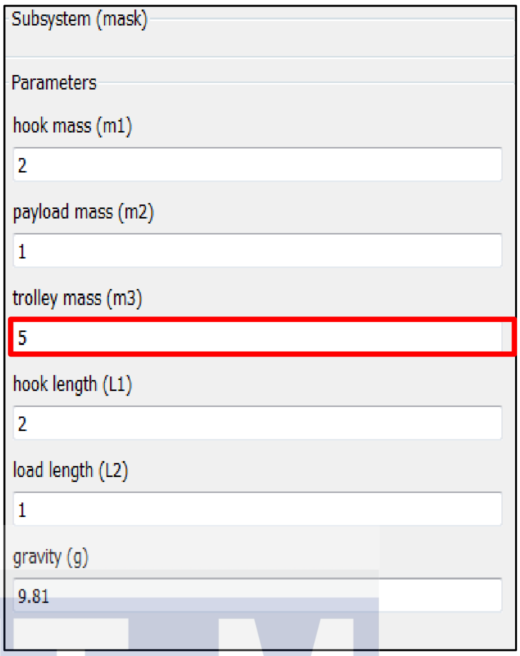

(b)

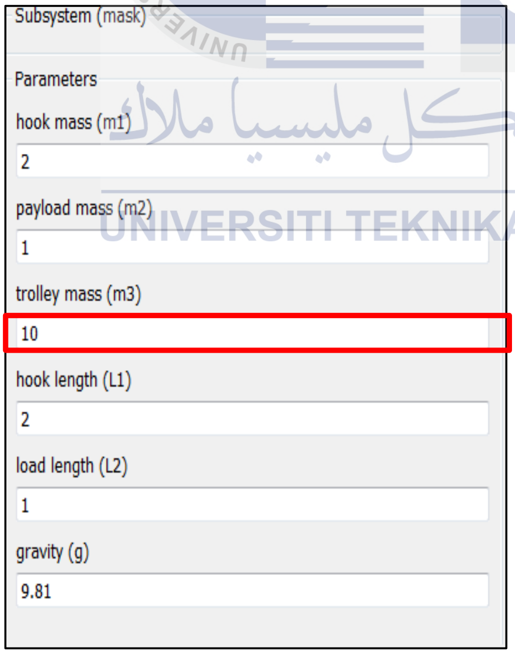

(c)

Figure 5.32: Different Trolley Mass Setting:

(a) 1 kg (b) 5 kg (c) 10 kg

Finally, analysis is completed by increasing the mass of trolley. Trolley mass is added by 1 kg, 5 kg and 10 kg to analyze the characteristic of DPGCS. Figure 5.33 shows the desired position of 5 N input forces that has been set. The Figure below (Figure 5.34, Figure 5.35 and Figure 5.36) shows clearly all the response involved such as the trolley displacement, hook and load oscillation. Other parameters are still maintained as described in the Table 4.1.

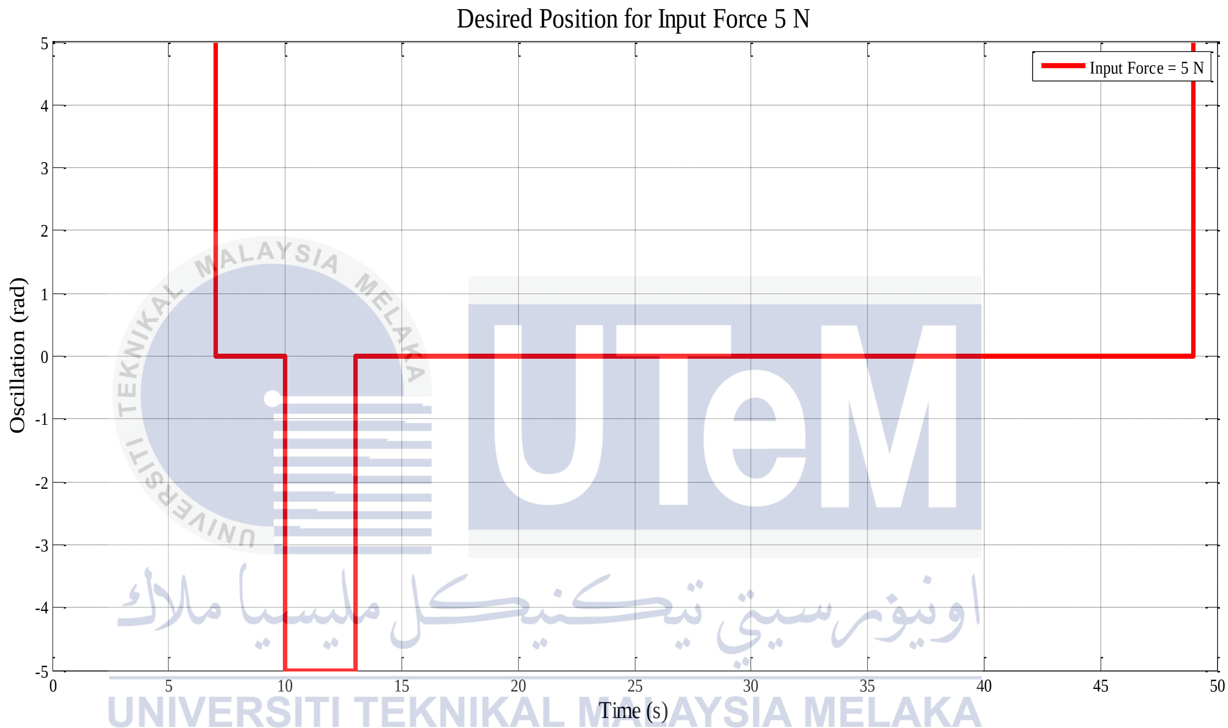

Figure 5.33: Bang-bang Input (5 N) for Different Trolley Mass

Table 5.16: Trolley Displacement with different Trolley Mass (*m3*)

Trolley Mass (kg)	Distance (m)
1	0.06391
5	0.02074
10	0.01135

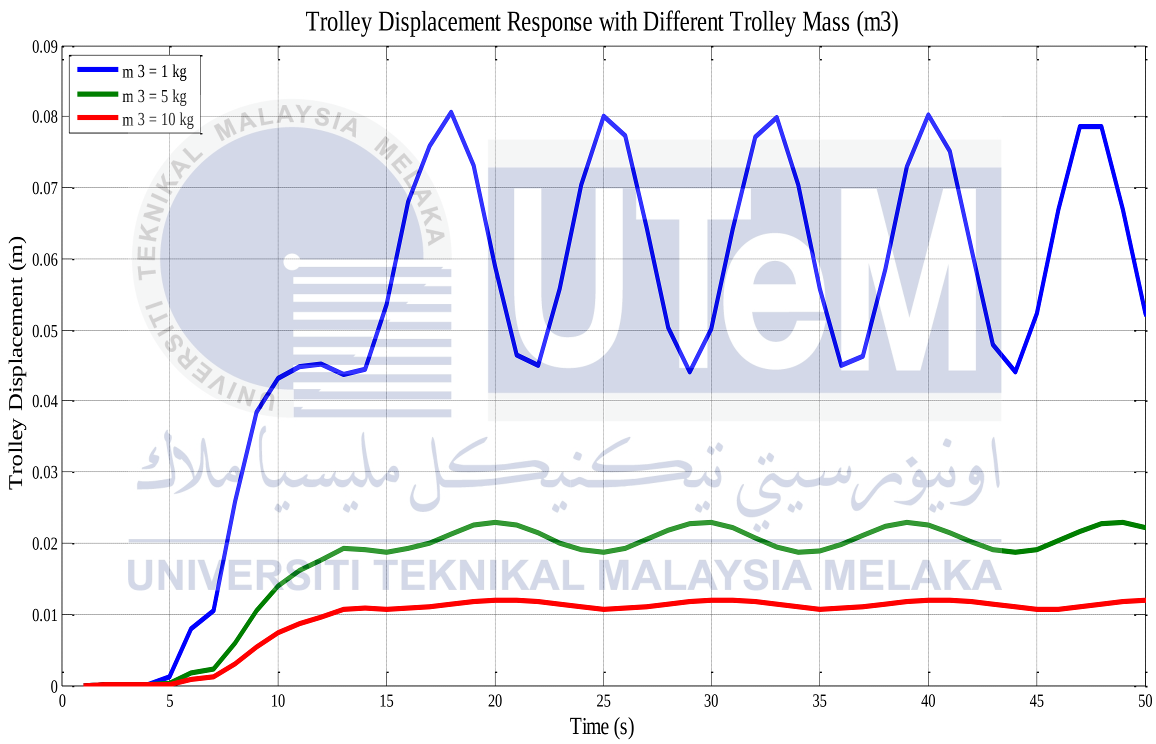

Figure 5.34: Response of Trolley Displacement with Different Trolley Mass (m3)

Table 5.17: Hook Swing Angle with different Trolley Mass (*m3*)

Trolley Mass (kg)	**Maximum Hook Swing Angle (x 10^{-3} rad)**
1	0.00723
5	0.00548
10	0.00411

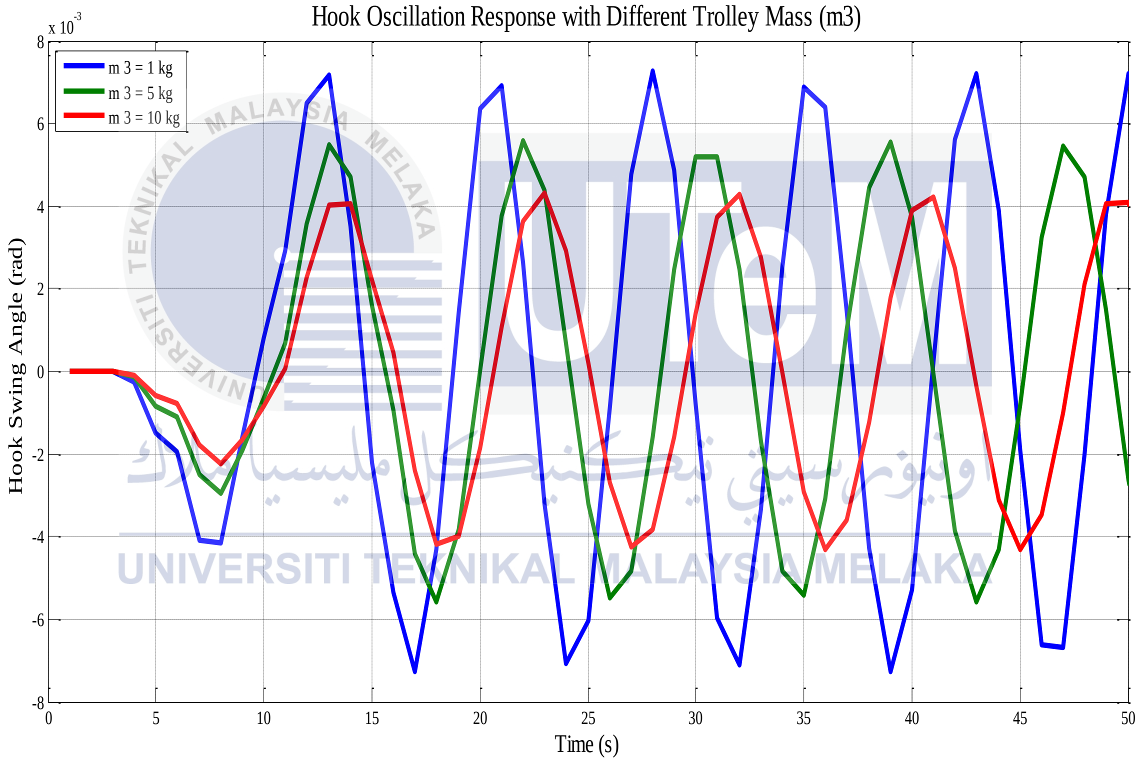

Figure 5.35: Response of Hook Oscillation with Different Trolley Mass (m3)

Table 5.18: Payload Swing Angle with different Trolley Mass (*m3*)

Trolley Mass (kg)	**Maximum Payload Swing Angle (x 10^{-3} rad)**
1	0.03597
5	0.01271
10	0.00682

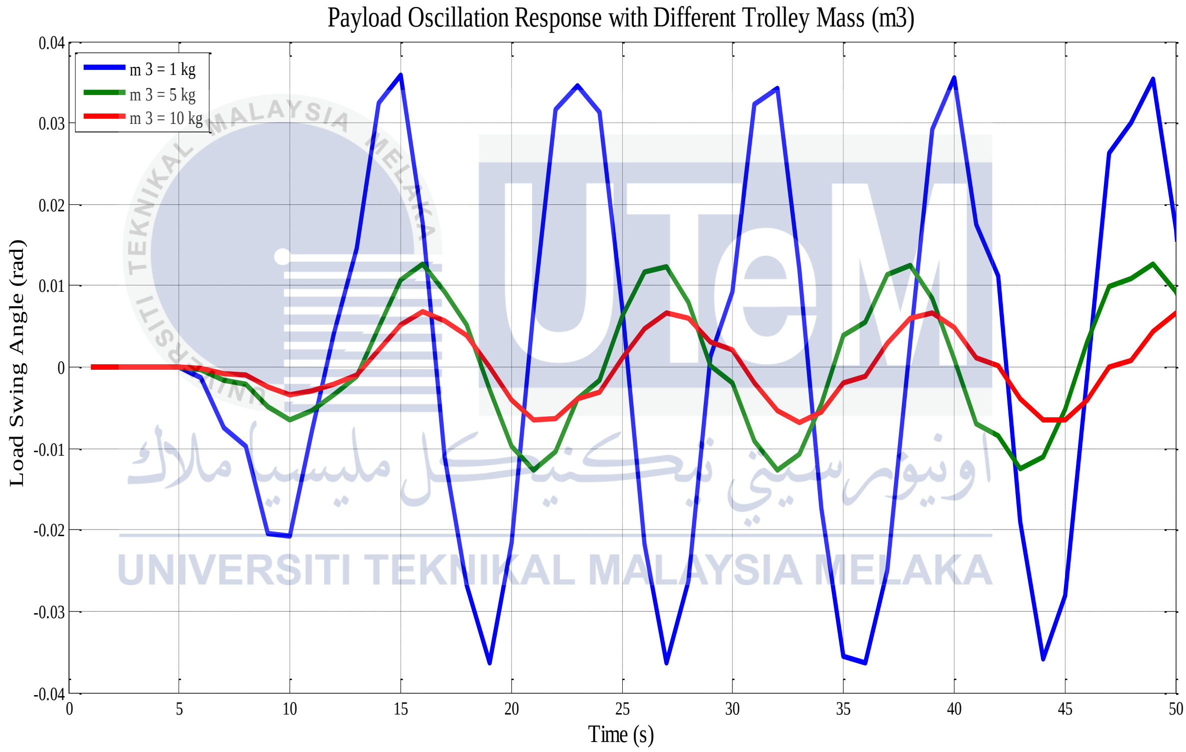

Figure 5.36: Response of Payload Oscillation with Different Trolley Mass (m3)

Table 5.19: Behavior of Double Pendulum Gantry Crane Model with Different Parameter Setting

		TROLLEY DISPLACEMENT, *x*		**HOOK OSCILLATION, θ_1**			**PAYLOAD OSCILLATION, θ_2**		
Parameters	Variable values	Distance, *x* (m)	Frequency, *f* (Hz)	Max. Angle, θ_1 (x 10^3 rad)	Frequency, *f* (Hz)	Period, m one cycle T(s)	Max. Angle, θ_2 (x 10^3 rad)	Frequency, *f* (Hz)	Period, m one cycle T(s)
Input Force, *N*	1.0 N	0.0009	0.1316	0.00028	0.1020	9.8	0.00058	0.1010	9.9
	3.0 N	0.0075	0.1316	0.00240	0.1042	9.6	0.00469	0.0901	11.1
	5.0 N	0.0207	0.1316	0.00630	0.1111	9.0	0.01275	0.0870	11.5
	7.0N	0.0410	0.1316	0.00960	0.1136	8.8	0.02160	0.0833	12.0
	10.0 N	0.0830	0.1316	0.01500	0.1124	8.9	0.03370	0.0794	12.6
Hook Length, L_1	1.15 m	0.01552	0.1176	0.00571	0.1111	9.0	0.00954	0.0813	12.3
	1.35 m	0.01564	0.1031	0.00588	0.1063	9.4	0.00931	0.0787	12.7
	1.55 m	0.01573	0.1000	0.00560	0.1010	9.9	0.00913	0.0775	12.9
	1.75 m	0.01581	0.0980	0.00519	0.0962	10.4	0.00895	0.0763	13.1
	2.00 m	0.01597	0.0901	0.00490	0.0926	10.8	0.00810	0.0725	13.8
Load Length, L_2	0.15 m	0.02082	0.1087	0.00211	0.0833	12.0	0.00661	0.0769	13.0
	0.35 m	0.02084	0.0758	0.00393	0.0535	18.7	0.01141	0.0403	24.8
	0.55 m	0.02087	0.0654	0.00457	0.0426	23.5	0.01185	0.0400	25.0
	0.75 m	0.02093	0.0565	0.00511	0.0386	25.9	0.01290	0.0373	26.8
	1.00 m	0.02097	0.0508	0.00610	0.0360	27.8	0.01275	0.0341	29.3
Hook Mass, m_1	1 kg	0.01782	0.0971	0.00772	0.0535	18.7	0.01110	0.0521	19.2
	3 kg	0.01376	0.1075	0.00636	0.0588	17.0	0.00741	0.0565	17.7
	5 kg	0.01144	0.1205	0.00554	0.0606	16.5	0.00499	0.0606	16.5
	7 kg	0.00962	0.1220	0.00329	0.0667	15.0	0.00341	0.0645	15.5
	10 kg	0.00742	0.1316	0.00285	0.0725	13.8	0.00267	0.0704	14.2

Payload Mass, m_2	1 kg	0.02086	0.0781	0.00598	0.0599	16.7	0.01280	0.0565	17.7
	3 kg	0.01578	0.0909	0.00504	0.0613	16.3	0.00968	0.0602	16.6
	5 kg	0.01251	0.1010	0.00423	0.0633	15.8	0.00741	0.0633	15.8
	7 kg	0.01045	0.1111	0.00356	0.0658	15.2	0.00559	0.0662	15.1
	10 kg	0.00838	0.1234	0.00309	0.069	14.4	0.00382	0.0730	13.7
Trolley Mass, m_3	1 kg	0.06391	0.1149	0.00723	0.0943	10.6	0.03597	0.0862	11.6
	3 kg	0.03125	0.1010	0.00649	0.0901	11.1	0.01881	0.0752	13.3
	5 kg	0.02074	0.0952	0.00548	0.0862	11.6	0.01271	0.0735	13.6
	7 kg	0.01566	0.0877	0.00472	0.0833	12.0	0.00949	0.0725	13.8
	10 kg	0.01135	0.0862	0.00411	0.0820	12.2	0.00682	0.0704	14.2

5.4 Results and Discussion

Data as illustrated in Table 5.4 shows in more detail on all changes that occurred when setting different parameters to the system. Observations are based on the criteria needed that are trolley displacement, frequency of hook, frequency of load and maximum oscillation of hook and payload.

Observation can be seen as in Figure 5.36. The distance of trolley is affected by the input force. Greater distances can be achieved with a trolley with increasing input force. In addition, the two frequencies are also affected by the input force. Contrary to hook frequency, the frequency of payload plotted that by increasing the input force the frequency are decreased. Furthermore, maximum of hook oscillation and the maximum of payload oscillation are increased when increasing the input force.

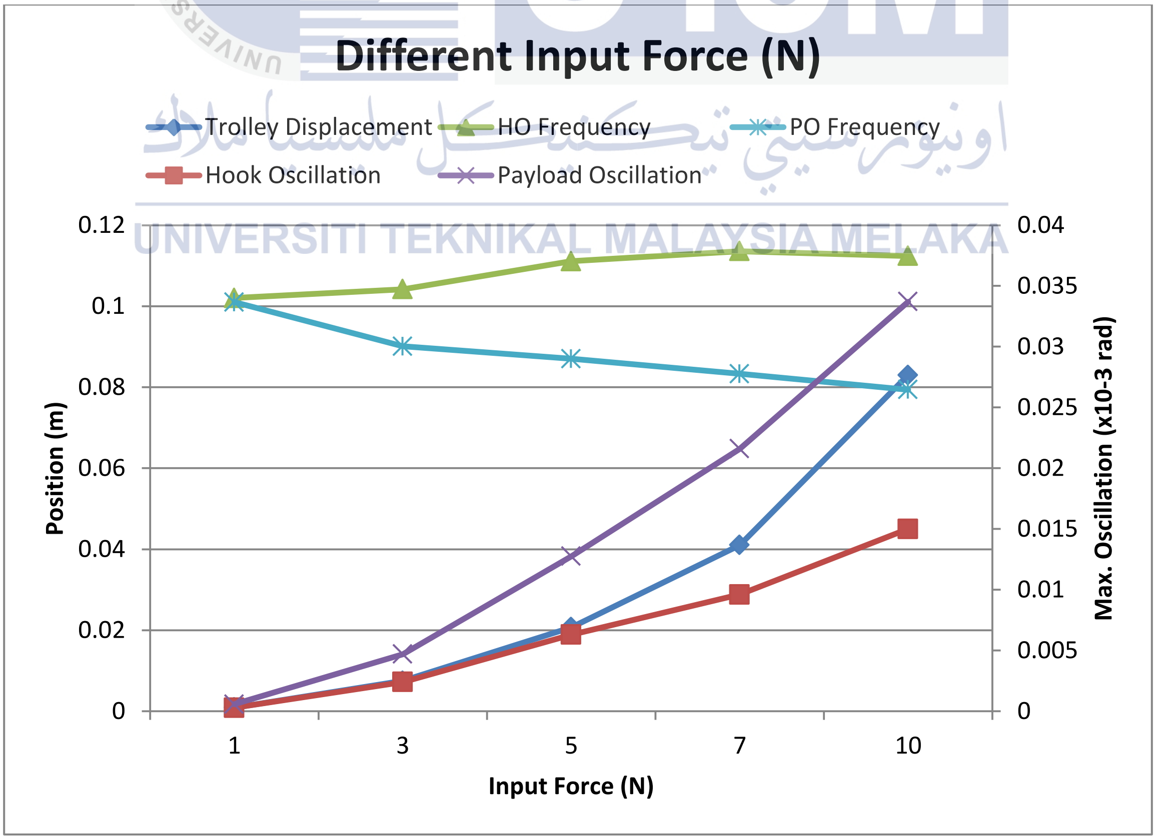

Figure 5.37: Different Input Force (*F*)

Figure 5.37 shows that the distances of trolley are not much affected by increasing the length of hook. The hook and the load oscillation frequency depends on the length of the hook where shorter the length, the greater the frequency is obtained. However, hook frequency is greater comparing the frequency of the payload. Maximum oscillation of hook and payload can be seen that it decreases as the length of the hook is increased.

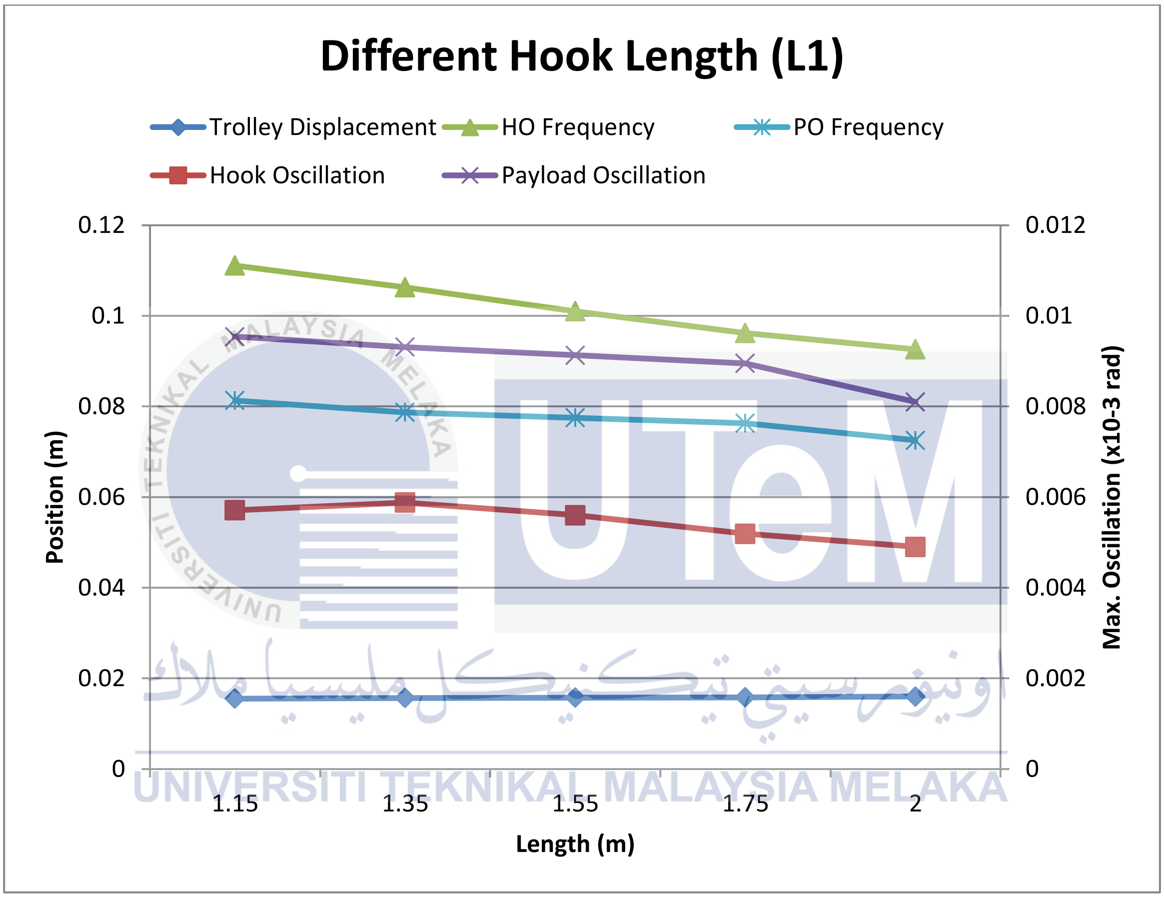

Figure 5.37: Different Hook Length (*L1*)

Figure 5.38 shows the distance of the trolley is not affected much when the length of the load increases. Similar to the different hook length, both the frequency of oscillation is also highly dependent on the length of the load. It can be seen that the shorter length of the load, the greater the frequency is achieved. Maximum oscillation of hook is greater when the length of load is increased. Maximum oscillation of payload can also see that it is even greater when the longer hook length.

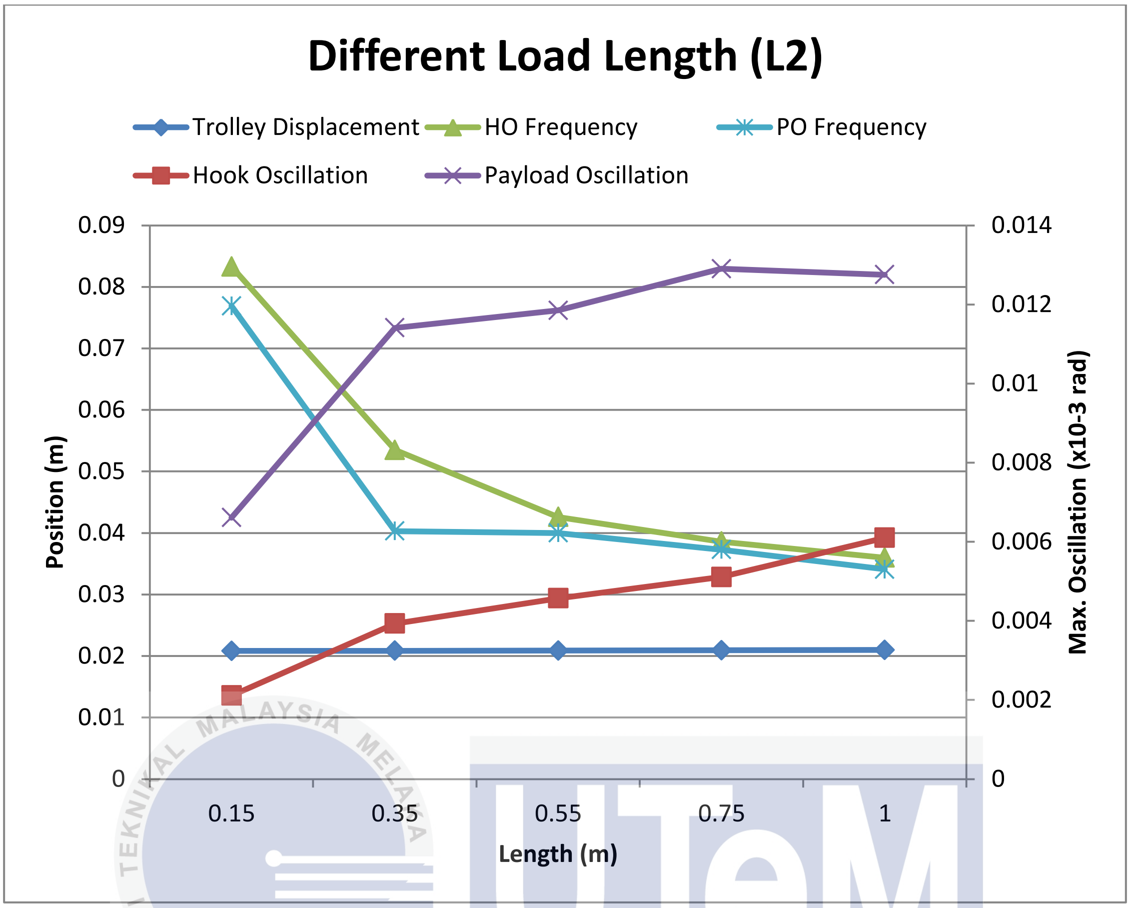

Figure 5.38: Different Load Length (*L2*)

In Figure 5.39, it shows the effect of setting the hook with the different mass. From the observation, trolley distance is affected when the mass of hook increased. Larger mass hook is applied; the lower distance can be achieved by the trolley. In addition, the frequency of the system is dependent on the hook mass. The larger the hook mass, the greater the frequencies were plotted. In this figure, the two frequencies showed a similar pattern of frequencies. However, the maximum oscillation of hook and payload are decrease when the hook mass increases.

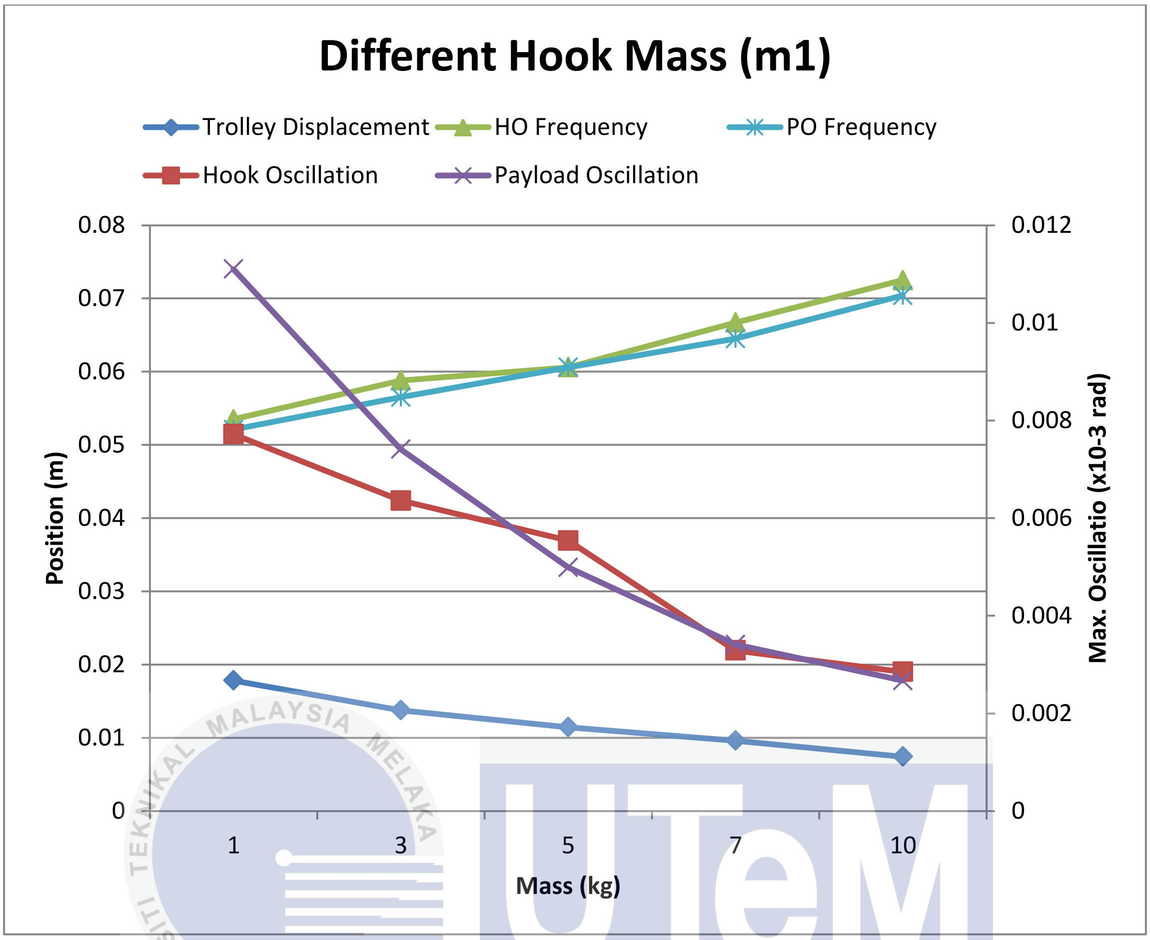

Figure 5.39: Different Hook Mass (*m1*)

Next, Figure 5.40 illustrates the different payload mass settings. Increasing the payload mass is given effect to the system, this can be seen in the distance of trolley that has been affected by increasing the payload mass. It shows that the distance of trolley was shorter when increase the payload mass. The system frequency also depends on the mass of payload. The greater the frequency is plot as the mass load increases. Both the frequency also has the same pattern of frequencies. In addition, the maximum oscillation of hook and payload are decreases when the mass load increases.

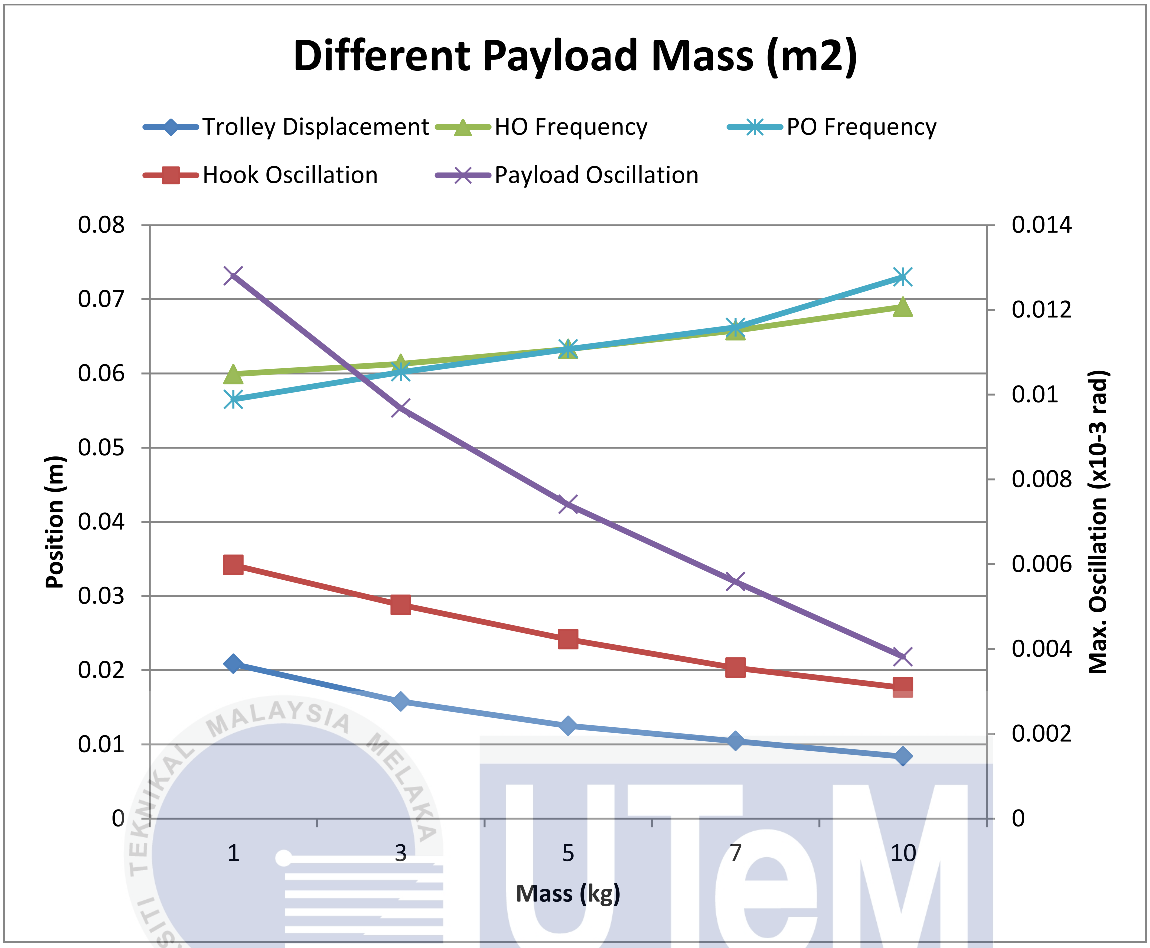

Figure 5.40: Different Payload Mass (*m2*)

Finally, Figure 5.41 states that the distance of a trolley is affected by various mass. Greater mass itself, the lower distance can be achieved by the trolley movement. Frequency of DPGCS is dependent on the mass of the trolley which the larger mass is applied, lower the frequencies. Besides that, maximum oscillation of payload is also decreased.

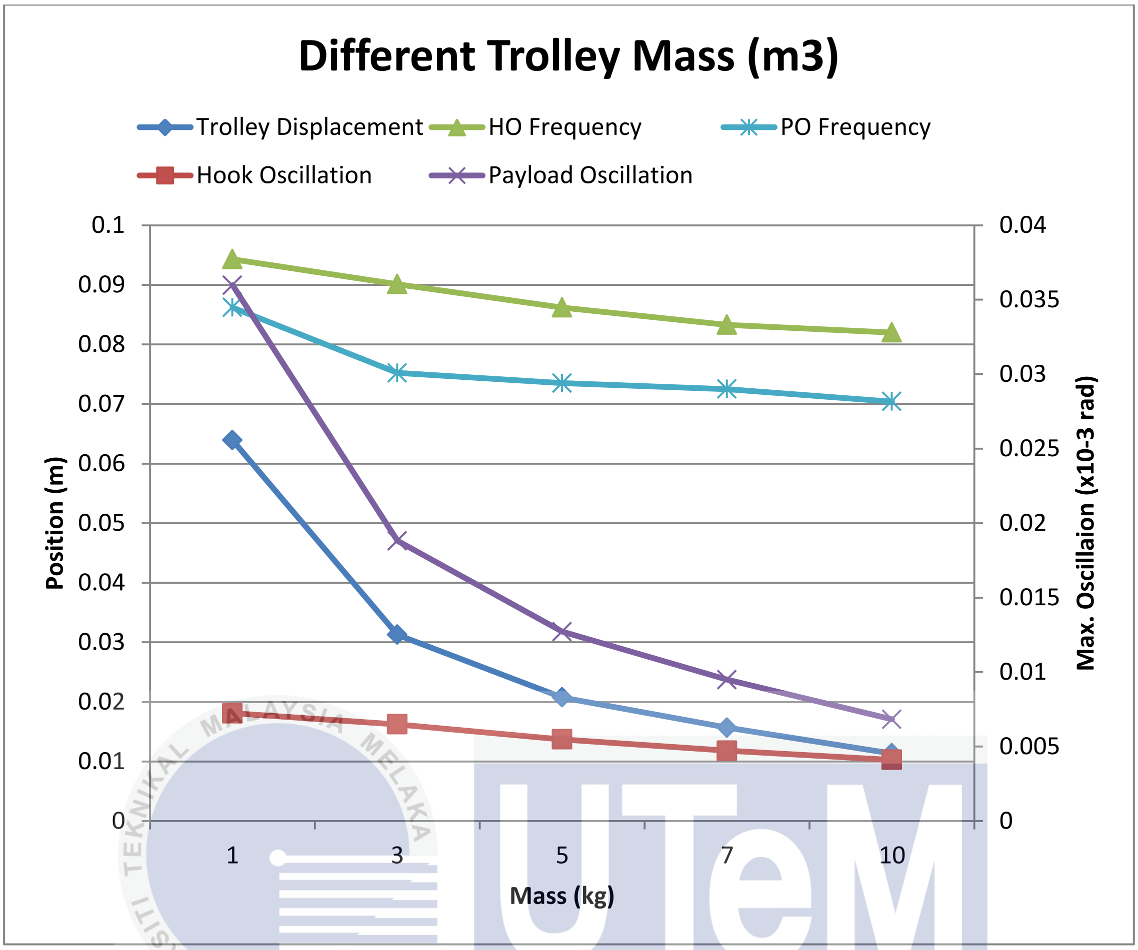

Figure 5.41: Different Trolley Mass (*m3*)

CHAPTER 6

CONCLUSION AND RECOMMENDATION

6.0 Overview

This chapter will be concluded overall the project done after the result or outcome of a response performance. The conclusions are excellently presented.

6.1 Conclusion

DPGCS is a complex system where this system has the characteristics of nonlinear. In this project, there are two conclusions will be provided in the first phase and second phase. For the first phase, it is describes about the analysis of DPGCS behavior which explains the response generated by increasing the payload mass (*m2*). Second phase describes more on analysis of DPGCS behavior with various parameters setting. The parameters involved is on input force (*F*), length of hook (*L1*), length of load (*L2*), hooked mass (*m1*), payload mass (*m2*) and trolley mass (*m3*).

6.1.1 Conclusion of First Phase: Analysis of DPGCS Behavior

The investigation of the development of a dynamic model of a DPGCS has been presented. A dynamic model of the DPGCS has been developing by using a Lagrangian Method. The simulation of the system has been simulated with bang-bang input force. The trolley displacement, hook oscillation and payload oscillation responses of the DPGCS have been obtained and analyzed in time and frequency domains. In addition, the effects of payload on the dynamic characteristic of the system by increasing the payload weights are discussed and studied. The performance results are clearly presented.

6.1.2 Conclusion of Second Phase: Analysis of DPGCS Behavior with Various Parameters Setting

Investigation of dynamic models DPGCS was presented with more emphasis on a more detailed analysis. Dynamic model of the DPGCS has been deeply investigated by using various system parameters of the system. Observation based on six criteria needed which is hook and payload length, input force, payloads mass, hook mass and trolley mass. System response such as trolley displacement, hook oscillation and payload oscillation are analyzed. Besides, the response and performance of DPGCS analysis has already discussed and stated clearly.

6.2 Recommendation

This project has been stated the effects of payload on the dynamic characteristic of the system by increasing the payload weights. These analyses are very beneficial for development of DPGCS for controller development and control algorithms. This project was continued by making a comparative study on trolley displacement, hook and load swing angle as well as the several of both length and input forces.

For future work, DPGCS will extend the approach of analysis in more detail by implement the controller and control algorithms such as fuzzy or other controller into the system so that it can control the payload swing with better result. Besides that, implementation by using optimization techniques also can be done to provide better system. In addition, implementation of experimental studies using different types of cranes (tower cranes or rotary cranes) can be applied to assist in development of control algorithm.

REFERENCES

[1] Le Anh Tuan & Soon-Geul Lee. Sliding Mode Controls of Double-Pendulum Crane Systems. *Journal of Mechanical Science and Technology* 27 (6) (2013) 1863~1873, 2013, January 23.

[2] Hazriq Izzuan Jaafar, Z. Mohamed, J.J. Jamian, Amar Faiz Zainal Abidin, Anuar Mohamed Kassim & Z. Ab Ghani. Dynamic Behavior of a Nonlinear Gantry Crane System. *The 4th International Conference on Electrical Engineering and Informatics* (ICEEI 2013)

[3] W.O'Connor & H. Habibi. Gantry Crane Control of a Double-Pendulum, Distributed-mass Load, Using Mechanical Wave Concepts. *UCD School of Mechanical and Materials Engineering*, UCD Belfield, Dublin 4, Ireland, Mech. Sci., 4,251-261, 2013, doi:10.5194/ms-4-251-2013.

[4] M. N. A. Zohari, M. Z. Mohd Tumari, M. S. Saealal, K.H. Ghazali & M.S. Ramli. Practical Sway Motion Control for Double Pendulum-Type Overhead Crane System. *International Journal on Smart Sensing and Intelligent Systems, Vol. 5.* No. 2, June 2012.

[5] Kimberly Curth, Car Smashed as Crane Topples onto Road. Available at: http://www.craneaccidents.com/2013/05/report/13016/ [Retrieves in May 21 2013]

[6] Mahdieh Adeli, Hassan Zarabadipour, Seyedeh Hamideh Zarabadi, & Mahdi Aliyari Shoorehdeli. Anti-Swing Control for a Double-Pendulum-Type Overhead Crane Via Parallel Distributed Fuzzy LQR Controller Combined with Genetic Fuzzy Rule Set Selection. *2011 IEEE International Conference on Control System, Computing and Engineering.* (2011)

[7] R.M.T. Raja Ismail, M.A. Ahmad, M.S. Ramli, R.Ishak, & M.A.Zawawi, Dynamic Modelling of a Double-Pendulum Gantry Crane System Incorporating .Payload, *Proceedings of Forth Global Conference on Power Control and Optimization.* ATP Conf.Proc.1337, 118-122 (2011); doi:10.1063/1.3592452, 2011 American Institute of Physics.

[8] Mahdieh Adeli, Hassan Zarabadipour, & Mahdi Aliyari Shoorehdeli. Anti-Swing Control of a Double-Pendulum-Type Overhead Crane Using Parallel Distributed Fuzzy LQR Controller. *International Journal of the Physical Sciences Vol. 6(35),* pp. 7850-7856, 23 December 2011, doi: 10.5897/IJPS11.1587, ISSN 1992-1950 ©2011 Academic Journals.

[9] Ajeya Karajgikar, Joshua Vaughan, & William Singhose. Double-Pendulum Crane Operator Performance Comparing PD-Feedback Control and Input Shaping. *Advances in Computational Multibody Dynamics MULTIBODY DYNAMICS 2011.* ECCOMAS Thematic Conference Brussels, Belgium, 4-7 July 2011

[10] Chen Li-jie. Research on the Non-Linear Dynamical Behavior of Double-Pendulum. *2011 International Conference on Mechanical Science, Electric Engineering and Computer.* August 19-22, 2011, Jilin, China

[11] M.A. Ahmad, M.S. Saealal, R.M.T. Raja Ismail, M.A. Zawawi, A.N.K. Nasir, & M.S. Ramli. Single Input Fuzzy Controller with Command Shaping Schemes for Double-Pendulum-Type Overhead Crane. *Global Conference on Power Control and Optimization, Kuching, Malaysia.* 2-4, December 2010.

[12] Joshua Vaughan, Ehsan Maleki, & William Singhose. Advantages of Using Command Shaping Over Feedback for Crane Control. *2010 American Control Conference.* Marriott Waterfront, Baltimore, MD, USA (June 30-July 02, 2010)

[13] R.M.T. Raja Ismail, M.A. Ahmad, M.S. Ramli, & F.R.M. Rashidi. Nonlinear Dynamic Modelling and Analysis of a 3-D Overhead Gantry Crane System with Payload Variation. *Faculty of Electrical and Electronics Engineering Universiti Malaysia Pahang.*

[14] Dian-Tong Liu, Wei-Ping Guo, & Jian-Qiang Yi. Composite Sliding Mode Fuzzy Control for Double-Pendulum-Type Overhead Crane. *Proceedings of the Fourth International Conference on Machine Learning and Cybernetics.* Guangzhou, 18-21 August 2005.

[15] Dian-Tong Liu, Wei-Ping Guo, Jian-Qiang Yi, & Dong-Bin Zhao. Double-Pendulum-Type Overhead Crane Dynamics and Its Adaptive Sliding Mode Fuzzy Control. *Proceedings of the Third International Conference on Machine Learning and Cybernetics.* Shanghai, 26-29 August 2004, ©2004 IEEE.

[16] A brief of lifting gantries. Available at: http://www.cranestodaymagazine.com/features/a-brief-history-of-lifting-gantries/ [Retrieves in November 1 2000]

[17] Michael Kenison, & William Singhose. Input Sharper Design for Double-Pendulum Planar Gantry Crane. *1999 IEEE Conference on Control Applications.*

[18] William E.Singhose, & Samuel T. Towell. Double-Pendulum Gantry Crane Dynamics and Control. *Proceedings of the 1998 IEEE, International Conference on Control Applications,*.Trieste, Italy 1-4 September *1998.*

[19] M.A. Ahmad, R.M.T. Raja Ismail, M.S. Ramli, A.N.K. Nasir, N.M. Abd Ghani, & N.H. Noordin. Technique for Sway Control of a Double-Pendulum-Type Overhead Crane. *Control and Instrumentation Research Group (COINS), Faculty of Electrical and Electronics Engineering, Universiti Malaysia Pahang.* ISSN: 1473-804x online, 1473-8031 print, IJSSST Vol. 11, No.2.

APPENDIX A

GANTT CHART FOR FINAL YEAR PROJECT 1 (BEKU 4792)

TASK	September				October				November				December			
	W1	**W2**	**W3**	**W4**	**W5**	**W6**	**W7**	**W8**	**W9**	**W10**	**W11**	**W12**	**W13**	**W14**	**W15**	**W16**
	09-15	16-22	23-29	30-6	7-13	14-20	21-27	28-3	04-10	11-17	18-24	25-01	02-08	09-15	16-22	23-29
1 – Introduction																
Motivation																
Problem statement																
Objective of Project																
Scopes of Project																
2 – Literature Review																
Analysis of Information																
Synthesis of Information																
Evaluation of Information																
3 – Methodology																
Project Flow Chart																
Validity/Reliability of Data																
4 – Modeling of DPGCS																
Model of DPGCS																
Mathematical Modeling																

5 – Preliminary Result																
Model Simulation																
Analysis of DPGCS																
Synthesis of DPGCS																
Evaluation of DPGCS																
6 – Conclusion																
Conclusion (Phase 1)																

Explaination

Mid Semester Break

Final Year Project 1 Presentation

Final Exam Study Week

Task Done

APPENDIX B

GANTT CHART FOR FINAL YEAR PROJECT 2 (BEKU 4894)

TASK	Feb		Mar				Apr				May				June			
	W1	**W2**	**W3**	**W4**	**W5**	**W6**	**W7**	**W8**	**W9**	**W10**	**W11**	**W12**	**W13**	**W14**	**W15**	**W16**	**W17**	**W18**
	17-21	24-28	03-07	10-14	17-21	24-28	31-04	07-11	14-18	21-25	28-02	05-09	12-16	19-23	26-30	02-06	09-13	16-20
5 – Implementation, Result and Discussion																		
Model Simulation																		
Analysis of DPGCS																		
Synthesis of DPGCS																		
Evaluation of DPGCS																		
6 – Conclusion																		
Conclusion (Phase 1)																		
Conclusion (Phase 2)																		

Explanation

- Mid Semester Break
- Final Exam
- Final Year Project 2 Presentation
- Task Done
- Making Improvements the Final Report